NASA TECHNICAL TRANSLATION NASA TT F-15,532

THE DO 31 LANDING LOADS DURING VERTICAL LANDING AND THEIR CONSEQUENCES FOR FUTURE VSTOL DEVELOPMENTS

W. Schoernack

(NASA-TT-F-15532) THE Do 31 LANDING LOADS DURING VERTICAL LANDING AND THEIR CONSEQUENCES FOR FUTURE V/STOL DEVELOPMENTS (Scientific Translation Service) 56 p HC $5.75 CSCL 01C G3/02

N74-20668

Unclas 36287

Translation of "Die Landelasten der Do 31 bei Vertikallandungen und Folgerungen für zukünftige VSTOL Entwicklungen", Dornier-Werke G.m.b.H., Friedrichshaften (W.Ger.), BMVg-FBWT-72-24; 1972, 72 pp.

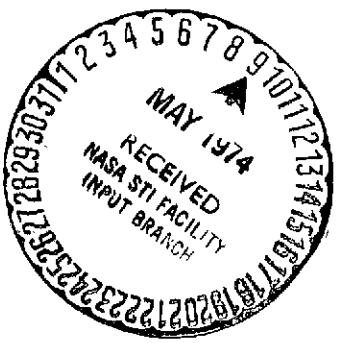

NATIONAL AERONAUTICS AND SPACE ADMINISTRATION
WASHINGTON, D. C. 20546 APRIL 1974

NOTATION AND ABBREVIATIONS:

A	kp	Lift force
A, B	-	Exponent (not defined more closely)
e_x, e_y, e_z	-	Reaction force factors ($e = 2P/G$), referred to one undercarriage side
f	mm	Shock absorbing strut stroke
G	kp	Landing weight of the aircraft
$g = 9{,}81$	m/s^2	Acceleration of gravity
P_x, P_y, P_z	kp	Reaction forces which apply to one undercarriage unit
S	kp	Engine thrust in vertical direction
S/G	-	Thrust/weight ratio
t	s	Time
U	kn, m/s	Trajectory velocity
w_s	m/s	Landing-sinking velocity (at touchdown
$\bar{w}_s$	m/s	Fictitious landing sinking velocity (See p.18)
γ	Deg	Trajectory angle relative to the horizontal
ϑ	Deg	Longitudinal inclination angle of aircraft
ϕ	Deg	Transverse inclination angle of aircraft

SUBSCRIPTS:

1	First landing shock
2	Second landing shock
02	Initial value at second touchdown
left	Left main undercarriage unit
right	Right main undercarriage unit

ABBREVIATIONS:

CL	Conventional landing
SL	Short landing
VL	Vertical landing
CTOL	Conventional takeoff and landing technique
STOL	Short takeoff and landing
VTOL	Vertical takeoff and landing technique

TABLE OF CONTENTS

THE DO 31 LANDING LOADS DURING VERTICAL LANDING AND THEIR CONSEQUENCES FOR FUTURE VSTOL DEVELOPMENTS

Wolfgang Schoernack

/ 5*

ABSTRACT: This report deals with the results of 83 vertical landings carried out during the Do 31 VSTOL Experimental Program.

In 23 landings undercarriage reactions as well as sinking speeds were measured, of the remaining 60 landings only sinking speeds could be evaluated. Undercarriage reaction factors and sinking speeds are plotted as frequency distributions and are discussed.

The result of the evaluation of the landing experiments can be summarized as follows: VTOL airplanes having a similar concept as the Do 31 and using manual control during the end of descent would experience considerably higher sinking speeds than conventional aircraft. It is remarkable that the frequency distribution of the sinking speeds is very severe, i.e., sinking speeds below 1 m/sec do not occur.

Furthermore, a typical jumping of the airplane after touchdown and a following second impact prove unfavorable, this second impact resulting in higher undercarriage reactions than the first one. The horizontal loads occurring with vertical landings are smaller than expected.

I. LANDING LOADS OF THE DO 31 FOR VERTICAL LANDINGS AND CONSEQUENCES FOR FUTURE VSTOL DEVELOPMENTS

1. Basic Aspects in the Design of Undercarriages for VSTOL Aircraft

If one compares the landing techniques of conventional landing, short landing and vertical landing aircraft, we find

---

* Numbers in the margin indicate pagination of original foreign text.

that there are two characteristic parameters which characterize the state of the aircraft during landing, which are noticeably different for the three different aircraft categories:

- The trajectory angle relative to the landing plane γ
- The trajectory velocity during the landing phase U

Both state variables have a decisive influence on the sinking velocity w_s perpendicular to the landing plane, which is the most important parameter for designing the undercarriage as far as shock absorption and strength are concerned. Therefore, they also influence the design of the fuselage structure.

The mutual dependence of the 3 parameters can be formally expressed as follows:

$$w_s \sim \gamma^A \cdot U^B$$

γ and U have the following opposing tendencies for the three aircraft categories: /6

	CTOL	STOL	VTOL
Trajectory angle γ	———	Increasing ——→	
Trajectory velocity U	———	Decreasing ——→	

Therefore, we cannot derive any tendency for the sinking velocity w_s from the above.

Numerous civil and military specifications have evolved from experiences collected over many years. However, even the newest version only consider aircraft with conventional landing techniques and rotary wing aircraft as examples of VTOL aircraft.

The safe sinking velocities specified in these publications for structural design are as follows:

- w_s = 2.15 (FAR 23) ... 3,05 (FAR 25) ... 4 m/s (MIL-A-8862A)

for conventionally landing aircraft or,

- w_s = 2,0 (FAR 29) ... 2,55 m/s (FAR 27)

for rotating wing aircraft.

Because there is no experience with STOL and VTOL aircraft, the prototype test facilities in the past had to specify landing parameters for experimental and prototype developments, which contained a certain safety margin. At the beginning of VSTOL development, a safe sinking velocity of w_s = 4.0 m/sec was assumed as a minimum, which was also used as a basis for the Do 31 design. / 7

In the meantime specification designs have been prepared in the United States and Great Britain over the last few years for STOL and VTOL aircraft, which already includes experience obtained with the first such aircraft. In the American design FAR.XX, a safe sinking velocity of 2.6 m/sec is required for vertical landings (VL) and no numerical value is specified for short landings (SL). In the design of the British aircraft agency ARB, published with the title "Provisional Airworthiness Requirements for Civil Powered-Lift Aircraft", a minimum value of w_s = 2.15 m/sec is required. Since there is no theoretically and experimentally based design value, a safe sinking velocity of w_s = 4.6 m/sec is required, and no distinction is made between SL and VL.

In other words there is no real agreement on these points. This is probably due to the fact that experience has been obtained in the United States with a prototype which is quite

different from the VTOL aircraft used in Great Britain for this purpose.

Another very important aspect of the undercarriage design is the question of the magnitude of the design side loads. For conventionally landing aircraft and most short landing aircrafts, the magnitude of the side load component during the landing shock depends primarily upon the sideslip angle and the oblique running properties of the tires. In the case of vertical landings, because of the slight side velocities, side loads will occur which are limited by the friction between the tires and the landing surface. In the most unfavorable case this means that the side load can have the magnitude of the vertical load.

The construction specifications restrict the side loads of conventionally landing aircraft between 25% (BCAR) and 40% (FAR) of the maximum safe vertical loads, because of the limitations mentioned above. For rotary wing aircraft, FAR 27 and 29 specify between 50 and 80% of the maximum reaction force as the design side force, depending on the loading case. The specification designs for VSTOL aircraft require 40% of the maximum vertical loads for VL (FAR XX) or 50% for VL and 75% for SL (ARB suggestion). This means that there are different points of view here as well. /8

2. Design of the Do 31 and Test Results

The Do 31 was designed for short and vertical landings with a safe sinking velocity of 4 m/sec. At the time, this value was assumed to be required and also the NATO specifications required this for a VSTOL fighter zone transport.

Because there was no experience with VTOL aircraft, the American military specification for rotary wing aircraft MIL-S-8698 was used for the side force design at the request of the prototype testing facility of the German air force (MBL). However, the requirement for a 50% side load in conjunction with a vertical load corresponding to a sinking velocity of w_s = 4 m/sec would have led to weight increases which could no longer be justified. Therefore, after agreement with the MBL had been reached, we defined a load case with w_s = 4 m/sec without a side load as well as a vertical landing case with w_s = 3 m/sec and a 50% side load.

During the VTOL experimental program, 100 vertical landings were carried out with the Do 31-E3.

The only accident which occurred involved the buckling of the main undercarriage legs and could be traced to a construction error of the locking mechanism. The permissible loading limits were not exceeded during this landing.

/ 9

Because of the harmless nature of this accident, we believe that we have a proof for the great safety of a VSTOL aircraft during the takeoff and landing phase.

Only the last phase of the sinking flight is important for the landing loads, that is, the vertical descent from a height between four and five meters, as well as the touchdown process.

The manual control of the touchdown process is made more difficult by the ground effects which occur (jet interference, recirculation), which leads to an increase in the sinking velocities. According to statements of the pilots, there was no way of influencing the sinking velocity.

The evaluation of the landing measurements shortly before contact with the ground therefore show a tendency for the sinking velocity to increase with decreasing height and a clear concentration at a value of 2 m/sec upon ground contact (Figure 17, 18).

The pilots were instructed to turn off the main engines at the instant of ground contact in order to avoid a jumping up of the aircraft. As experiments show (Figures 2, 3), it was never possible to avoid the rebound of the aircraft, probably because of the reaction times of the pilot and the engines. After the engine thrust had really dropped off, the second landing shock occurred with a strong loss in lift. The reaction forces were therefore larger during the second touchdown than for the first touchdown (Tables 2 and 3, as well as Figures 4 to 9) during most of the measured landings.

Unfortunately, it was not possible to evaluate the sinking velocities after the first ground contact. Also, the rebound height as well as the thrust variation cannot be determined in practice. This means that only qualitative interpretations of the motion can be made during the second shock. / 10

In the case of the vertical landings of the Do 31, we always recorded side accelerations between 0.1 and 0.3 g and the corresponding side loads in the undercarriage. Therefore, we do not require a higher degree of safety than for conventional aircraft.

The most important results of the Do 31 test can be summarized as follows, as far as the undercarriage is concerned:

- No comparison with rotary wing aircraft can be made
- Overall, the sinking velocities and the shock loads are extremely high compared with conventional landing techniques.
- The safe sinking velocities must be assumed to be higher than for conventional aircraft.
- The side loads which occur are not higher than for conventional aircraft.

3. Undercarriage Design for Future VSTOL Aircraft

The requirements on the undercarriage design of future VSTOL aircraft depend primarily on the sinking velocity changes caused by the ground effect and the possibilities of controlling them.

In all configurations with a negative ground effect, the conditions will be similar to those of the Do 31, if the touchdown process is controlled manually. /11

Only a real VTOL aircraft can have a special design of the undercarriage shock absorbers, which would avoid or reduce the rebound of the aircraft and therefore avoid or reduce a second jump. In most cases it is likely that future VSTOL aircraft must be capable of short takeoffs and landings or conventional takeoffs and landings, especially if these are transport aircraft.

Special touchdown automatic systems which would make it possible to preselect the touchdown velocity could bring about basic improvements in the magnitude of the safe sinking velocity, the shock loads and influence the rebound upon ground contact. It seems that it will be necessary to develop this touchdown automatic system for civilian applications in particular. This is required not only because of the undercarriage design, but also

it will result in simpler handling of the aircraft and higher passenger comfort. /12

II. EVALUATION AND RESULTS OF THE LANDING SHOCK MEASUREMENTS

1. Introduction

The design of the Do 31 provided an undercarriage arrangement with two main undercarriage units within the region of the two main engine gondolas at the wing, and a nose wheel unit. This arrangement led to relatively high main engine undercarriage strokes in conjunction with the high-wing configuration.

Because of the special construction characteristics, limiting loads for the dimensioning of a large part of the wing structure for the load case resulted in "conventional horizontal landing with wheel rotation shock" considering the dynamic amplification effects. This was based on the large torsion moments resulting from horizontal forces. In order to test the load assumptions and the structural calculations, especially for the dynamic loads and in order to provide experimental foundations for the calculation of such dynamic landing load cases, we installed measurement devices in the Do 31-E1, the first experimental aircraft equipped for conventional flight testing. With this, the following quantities were recorded and measured as a function of time during 14 landings, in addition to the normal measurement program which includes physical data:

- Forces in the main undercarriage in all coordinate directions.

- Shock absorbing strut strokes.

- Accelerations at the wing, fuselage, control surfaces and undercarriage.
- Shear stresses at a cross section of the inner wing.

The qualitative evaluation of all conventional landings carried out led to the realization that the load cases which had been assumed for the dimensioning could not be brought about during operation. The evaluation of two landings in [1] and [2] shows that the stresses caused by the undercarriage shock lie within the usual operational limits for conventional landings. /13

During the VTOL test with a second experimental aircraft Do 31-E3, which was completely equipped with lifting engines, we found that considerably higher landing sinking velocities and therefore higher vertical undercarriage shock forces were achieved than during the conventional landings, in the case of vertical landings controlled manually by the pilot. As we will see, we particularly notice the large effect of the rebound of the aircraft which occurred regularly after first contact with the ground with a subsequent new touchdown.

Since the pilot wants to reduce the rebound and wants to turn off the lifting engines as soon as possible after touchdown, in spite of the small sinking velocity, the shock force can be larger during the second touchdown than for the first touchdown. This is caused because the main thrust-weight ratio S/G is considerably smaller than one and in addition, the stroke has not yet been completely equalized during the second rebound.

Since there were no measurement installations for determining the undercarriage shock forces in the Do 31-E3, we first only determined the landing sinking velocities from the radio height

measurement in [4]. This was then presented in the form of a frequency distribution. This evaluation already showed that the sinking velocity level and therefore the loads which occur during operation are considerably higher for vertical landings than for conventional landings.

The measurement installation was expanded within the framework of collaboration with NASA on VTOL flight testing using the Do 31-E3. It became possible to measure the loads in the main undercarriage during vertical landings. For this purpose, the /14
main undercarriage of the E1 was exchanged and built into the E3 and contained strain gauge bridges for determining the undercarriage loads. After adaptation of the measurement installation, we measured 23 vertical landings during the course of the NASA test program (Figures 19 and 20).

It is the purpose of the present report to obtain information on the undercarriage stresses of jet-supported VTOL aircraft derived from these measurements.

In order to evaluate vertical shock forces during landing, we can state that the sinking velocity is the most important influencing parameter. The sinking velocity is difficult to measure and can only be measured inaccurately. Therefore, we use the force measurements to support and correct the measurement results. This was possible during the 23 landings for the reasons mentioned above, and for which we were able to obtain time variations of the reaction forces and side loads from the force measurements.

It was possible to evaluate the sinking velocity measurements from sixty additional vertical landings. This means that the statistical data on the vertical reaction forces were well founded,

so that they were included in the frequency distribution.

In order to consider the number of load changes, which is important for fatigue calculations, the second landing shock had to be included in the collection of sinking velocities by means of a fictitious sinking velocity.

2. Description of the Measured Variables

/15

2.1. Measurement of the Landing Shock Forces and Shock Absorber Stroke for the Main Undercarriage

The shock forces with components P_x, P_y, P_z which apply at the main undercarriage units are referred to an aircraft-fixed axis system. The positive directions of this system agree with the reference axes of the aircraft and are defined as follows (Figure 19):

x-direction:	Positive backwards
y-direction:	Positive starboard
z-direction:	Positive upwards

The shock forces apply at the wheel axis (P_x, P_z) or at the tire contact surface (P_y) and are measured using strain gauge bridges attached at suitable points of the undercarriage structure. They are calibrated. (Figure 20). The theoretical bases and the practical execution of the measurements (Skopinski method) are described in [1] and [5].

The shock absorber strokes are measured using potentiometers at the wheel control core.

2.2. Measurement of the Sinking Velocity and Trajectory Velocity of the Aircraft

The sinking velocity is measured with an electrical variometer connected with the radio height measurement device. During the NASA test flights, a radio height measuring device with a measurement range between zero and 360 feet was installed for the lower height range. For the preceding test flights, a radio /16
height measuring device with a measurement range between zero and 120 feet was installed. The measurement accuracy of the landing sinking velocity, which is influenced by ground roughness effects even for small horizontal velocities, is probably smaller during the NASA flights than during the preceding test flights.

The horizontal velocity is measured using the Dornier-Fluglog.

2.3. Measurement of the Acceleration

The accelerations in the three axis directions are measured using the acceleration transducers in the vicinity of the center of gravity. These acceleration measurements could only be used to a limited extent for evaluating the shock process because the transducers did not respond to short time acceleration peaks, such as occur for the undercarriage shocks, at least in the z direction. Acceleration transducers installed in the shock absorbers for measuring the z-accelerations could only be applied infrequently within the framework of this evaluation. For the same reason, it was not possible to evaluate acceleration measurements in the outer gondolas.

2.4. Measurement Installation

The Do 31 measurement installation is described in [3]. /17

The signals of the strain gauge bridges and acceleration transducers at the undercarriages or wing tips are recorded using the FM frequency multiplex system. The shock absorber stroke and the other flight measurement data of interest are measured using the time multiplex system.

/ 18

3. TEST EVALUATION

3.1. Evaluation of the Landing Shock Forces

The force components P_x, P_y, P_z measured using strain gauge bridges along the left and right main undercarriage sides are determined from analog recordings using the calibration coefficients given in [5]. It was not possible to have a digital output of these measurement values because the digitalization program provided for this for frequency modulated measurement data could not be used. However, the evaluation of the analog recordings was appropriate for the requirements, even though this required more time and even though the accuracy was lower.

The components P_z (vertical force) and P_x (horizontal force) in the aircraft/fixed coordinate system were determined from a calibrated strain gauge bridge, containing strain gauges in the the wheel axis. The P_x measurement bridge at the rear undercarriage dropped out after the first landing measurement.

Since we did not obtain any useful results using the ultimate measurement installation for measuring P_z and P_x using a combination of three strain gauges, it was not possible to determine P_x at the left undercarriage side, except for one landing (Experiment No. 220).

This latter statement is inconsequential for the information obtained from these measurements, because the forces P_x are necessarily small for vertical landings with small forward velocities.

The side force P_y was determined using the coefficients obtained from the calibration from the combination of two strain gauge bridges each. A comparison of the side forces with the associated side accelerations showed that apparently the sign of the y force of the left undercarriage was wrong because of an error in the installation of the measurement installation. This error was corrected when the results were evaluated and processed. /19

From the analog recordings of P_z it is obvious that the aircraft and the main undercarriage rebounds after the first touchdown from the ground in all of the 23 measured landings. The shock forces P_z during the second touchdown are greater than for the first touchdown for all of these landings. For this reason, the undercarriage shock forces were determined separately for the first and second landing shock.

3.2. Evaluation of the Landing and Sinking Velocity /20

From the measurement data of the radio height measuring device or the connected electrical variometer, we find sinking velocity values which fluctuate more or less and sometimes increase in the vicinity of the ground. The following influences could be responsible for these phenomena:

- The signals of the radio height measuring device designed for the 360 foot measurement range are disturbed by ground roughness effects during the vertical landings carried out with relatively small forward velocities.

This can result in a considerable scatter of the signals towards the ground because of the large measurement range of the radio height measuring device.

- The engine thrusts did not remain constant during the descent. Because of hot gas circulation and jet interference, they can decrease in an irregular fashion in the ground effect zone and cannot be controlled by the pilot in order to obtain a uniform, unaccelerated final descent. This means that in this region, the main thrust-weight ratio S/G is already smaller than 1 and the sinking velocity increases.

This means that the determination of the landing sinking velocity w_s from this radio height measurement contains some degree of uncertainty. In contrast to this, the measurement of the landing shock forces P_y, P_z and their determination from analog recordings can be considered to be relatively accurate. In order to support the experimental determination of the landing sinking velocity w_s, we carried out motion calculations of the landing process on the computer in parallel with the test evaluation. We used the known design data of the undercarriage system and determined the shock forces P_z as a function of the sinking velocity w_s, and we assumed a thrust-weight ratio of S/G=1, as well as the average values of the true landing weights and landing inclination angles. Figure 1 shows P_z plotted as a function of w_s for G = 18500 kp and $\theta = 3°$ as obtained from this calculation. The calculation applies for a symmetric landing, i.e. for equal shock loads on the left and right sides of the undercarriage. /21

Since the shock forces P_z are not the same on the left and right sides for most of the measured landings, the true resistance

parallel to the ground cannot be taken into account in the calculation and because S/G is already smaller than one for the first touchdown, of course the determination of the landing sinking velocity of the aircraft from the measured shock forces P_z will be inaccurate using the impact calculations mentioned above.

The approximate determination of the sinking velocity w_s for the first touchdown from measured impact forces P_z according to the method given above can be looked upon as adequate for a statistical evaluation of the measurement results in the form of frequency distributions.

As already mentioned, the analog traces of P_z show that the aircraft rebounds after touchdown and lifts away from the ground during all 23 measured landings.

For the subsequent second touchdown, the analog recordings have a much flatter increase of P_z which decreases over the shock time, compared with those of the first touchdown. Since the shock forces P_z are greater compared to the measured sinking velocities than for the first touchdown, from this we may conclude that the lifting thrust-weight ratio S/G is much smaller for the second landing shock than for the first one. From this it follows that the lifting engines are turned off more or less rapidly by the pilot after the first ground contact. Since /22
there are no sufficiently differentiated lifting thrust data available for the landing phase, it is not possible to determine the most important parameters S/G besides the sinking velocity w_s during the second landing shock within the framework of this paper, which could then be used for a statistical frequency evaluation. During the second landing shock we find that the shocks during the second landing shock have not been completely extended by the springs when the second touchdown occurs, according to measurements of the shock absorbing struts. This is

expressed by an increase in the shock load. Four exceptions to this were measured.

Even though the sinking velocity w_{s2} during the second landing shock alone does not give any information on the shock forces if S/G is also not known, we nevertheless determined the values of w_{s2} from the sinking velocity measurement using the electrical variometer connected to the radio height measurement device. This was done in order to have a means of comparison. However, it is not possible to check or correct the measured values of w_{s2} as before using the measured shock forces when w_{s1} is determined. This is because the magnitude and variation of S/G are not available for the second landing shock.

In order to obtain a characteristic frequency representation by means of the sinking velocity alone during the second landing shock especially for the Do 31-E3, fictitious computered landing sinking velocities $\bar{w}_{s2}$ were determined using the shock calculation. This calculation satisfies the requirement that at S/G = 1 and for initially completely extended shock absorbing strokes, the measured shock forces P_{z2} during the second landing shock are approximately obtained, and are therefore comparable to w_{s1} for the first landing shock.

4. PRESENTATION OF RESULTS /23

4.1. Tabular Summary of the Measurement Results and Evaluation Results

Table 1 shows the following landing state variables for evaluating the shock forces:

- Landing weight G
- Trajectory velocity U
- Longitudinal inclination angle θ
- Transverse inclination angle ϕ
- Sink velocity for the first touchdown w_{s1}
- Sink velocity for the second touchdown w_{s2} and $\bar{w}_{s2}$, respectively.

The values of G are taken from the available weight summaries. The values of U, θ and ϕ are taken at the time of the first touchdown from the "quick look" data. The sinking velocity values w_{s1}, w_{s2} and $\bar{w}_{s2}$ are determined using the approximate method described before in Section 3.2.

Table 2 shows the undercarriage shock forces P_{x1}, P_{y1}, P_{z1} and the shock force factors e_{x1}, e_{y1}, e_{z1} determined from them (referred to G/2) as well as the shock absorbing strut strokes, f_1 at the left and right main undercarriage side during the first landing shock.

In the same way, Table 3 shows the shock forces P_{x2}, P_{y2}, P_{z2}, which result during the second landing shock, the shock factors e_{x2}, e_{y2}, e_{z2} as well as the shock absorbing strut stroke f_{o2} at the time of the second touchdown and the maximum value f_2 during the second landing shock. In experiment No. 234, we did not obtain any measured values for determining the shock absorbing strut strokes. The values of f_{02} in Table 3 show that for the landings considered, except for experiment No. 240, and on one side each for experiments No. 241 and 244, the shock absorbing strut was not completely extended at the time of the second touchdown.

The values of P_x, P_y and P_z assumed in Tables 2 and 3 are always maximum values, which do not always exactly coincide in time. /24

4.2. Graphical Presentation of the Measurement Results and Evaluation Results

Figures 2 and 3 show the time variation of the shock forces P_z and P_y of two typical landings. Figure 2 shows experiment No. 228 with the greatest P_z force during the first landing shock. Figure 3 shows experiment No. 243 with the largest P_z force during the second landing shock. There is a typical P_z variation for all 23 measured landings. Clearly we can see the lift off of the aircraft from the ground after the first landing shock and the subsequent second developed landing shock.

In order to compare the stresses of the Do 31 undercarriage according to P_z and P_y during the first and second landing shock encountered during the 23 measured vertical landings, Figures 4 to 9 show frequency distributions of the shock force factors e_{z1} and e_{z2} with a classification interval of $\Delta e_z = 0.3$. Figures 10 and 11 show frequency distributions of the shock force factors e_{y1} and e_{y2} with a classification interval of $\Delta e_y = 0.05$. The representations show that the operational stresses as measured by P_z and P_y are harder for the second landing shock than for the first landing shock. The maximum values of P_z and P_y do not always occur at the same time. / 25

Since the shock force P_z in an undercarriage depends primarily on the landing sinking velocity w_s for a constant S/G, the operational load values of P_z in general will be determined through the frequency distribution of w_s. This is why we determined comparable frequency distributions of w_s using the

values of P_z determined from experimental measurements:

In Figure 12 we show the frequency distribution of the landing sinking velocity w_{s1} for the first landing shock obtained from 23 vertical landings with a classification interval of Δw_s = 0.5 m/sec. In the same way, we show the frequency of the fictitious values $\bar{w}_{s2}$ for the second landing shock determined for S/G=1 from a numerical comparison.

Figure 14 gives in the usual manner the frequency of exceeding w_{s1} (during the first landing shock) per flight, as determined from 23 landings. Considering the fact that during these landings, two well developed landing shocks occurred (as though two landings were flown one after another for each flight), we find the exceeding frequency per flight given in Figure 15 for a fictitious landing sinking velocity $\bar{w}_s$, assuming a thrust-weight ratio of S/G = 1 and the frequency distribution of w_{s1} according to Figure 12 and the frequency distribution of $\bar{w}_{s2}$ according to Figure 13.

Since the statistical information content of a frequency evaluation of the landing sinking velocity is relatively small as obtained from 23 flights, we included the frequency distribution of the landing sinking velocity w_{s1} determined earlier in [4] from 60 vertical landings, in order to have a more comprehensive evaluation. These 60 vertical landings were carried out during the Do 31-E3-VISTOL basic testing programs. However, this extended evaluation was restricted to the landing sinking velocity w_{s1} (first touchdown), because for these landings, no undercarriage shock forces were measured. Consequently we do not have any experimental data on the magnitude or existence of a second well-developed touchdown shock during these landings.

Figure 16 shows the frequency distribution of the landing sinking velocity w_{sl} was determined [4] from 60 vertical landings / 26 during the Do 31-E3-VSTOL basic testing program. These values were determined graphically from the radio height measurement (measurement range from 0 - 120 feet).

From the combination of the frequency distributions of w_{sl} according to Figure 12 (from 23 landings during the NASA test program) and Figure 16 (from 60 landings of the basic testing program) we find the frequency distribution of w_{sl} from a total of 83 vertical landings of the Do 31-E3 as shown in Figure 17. The frequency distributions w_{sl} in Figures 12 and 16 show that the landing sinking velocity level is higher on the average during the 23 landings carried out during the NASA test program than for the 60 landings carried out during the basic testing program. It should be noted that during the 60 landings performed during the basic testing program, there was no check of the sinking velocity values determined from the radio height measurement by means of shock force measurements.

Figure 18 shows the exceeding frequency w_{sl} per flight which results from the frequency distribution w_{sl} according to Figure 17 and from 83 vertical landings with the Do 31-E3. As a comparison we also show the exceeding frequencies according to the American military specifications MIL-A-8866 for conventional aircraft landing on airports. The dashed lines refer to training aircraft and the dash and dot lines correspond to normal military aircraft of other types. Therefore, Figure 18 shows that the sinking velocity level during the vertical landings of the Do 31-E3 is considerably higher than for conventional landings. This is shown even more clearly in Figure 15, because for example during the 23 vertical landings measured during the NASA test program, there were two well developed landing shocks which occurred per flight because of the rebound after the first touchdown shock.

In most of the 23 landings which could be evaluated in this regard, the shock forces P_{z2} and therefore the comparable computed sinking /27 velocity $\bar{w}_{s2}$ were larger than for the first landing shock.

5. DISCUSSION AND EVALUATION OF THE RESULTS

One important result is the fact that for all 23 measured vertical landings, because the aircraft rebounded after the first touchdown, there was a second well developed landing shock and the shock forces P_z are greater than for the first landing shock for most of these landings. (Tables 2 and 3, Figures 4 to 9). The number of asymmetric landing shocks, for which P_z are not the same on the left and the right undercarriage sides, is greater for the second touchdown than for the first touchdown (Tables 2 and 3). The true sinking velocity w_{s2} during the second touchdown is usually considerably smaller than for the first touchdown compared to the shock force P_z (Tables 1, 2 and 3). The large P_z forces during the second landing shock are conditioned by the fact that the power turns off the lifting engines as soon as possible after the first touchdown in order to avoid the rebound. This means that S/G during the second landing shock is substantially smaller than one. In addition, the shock absorbing struts are usually not completely extended when the second touchdown occurs, (fo2 in Table 3).

The fictitious sinking velocity values $\bar{w}_{s2}$ for the second touchdown which are comparable with the sinking velocity values w_{s1} which occur during the first touchdown, which were determined approximately from the shock forces P_z using shock calculations for S/G = 1 and initially completely deployed shock absorbing struts, are larger during the corresponding landings than the sinking velocity w_{s1} during the first touchdown (Table 1), just like the shock forces P_z. The rebound of the aircraft after the first touchdown shock and for the same undercarriage essentially

depends on the landing sinking velocity w_s. For the same sinking velocity, rebound is just as possible during conventional landings with A/G = 1 as during vertical landings with S/G = 1.

The reasons for the large rebound of the aircraft after touchdown are therefore the high landing sinking velocities w_{s1} which in our case are considerably higher than during conventional landings (Figures 14 and 18). /28

The operational stresses on the aircraft caused by the shock forces P_z are represented by the frequency distributions of the landing sinking velocities (Figures 12, 13 and 17) and the exceeding frequencies per flight (Figures 14, 15 and 18). These stresses are much greater for vertical landings of the Do 31-E3 than for the conventional landings. This is easily seen by the increased sinking velocity level for the first touchdown shock (Figures 14 and 18) and is amplified by the second touchdown shock (Figure 15).

The largest landing sinking velocity determined during a total of 83 landings is w_s = 3.4 m/sec and is therefore 15% smaller than the largest design sinking velocity of w_s = 4 m/sec, which was substituted for the Do 31 for the design landing weight of G = 21800 Kp.

The largest shock force P_z on one main undercarriage side determined from measurements of 23 vertical landings is the same for the first and second landing shocks and amounts to $P_{z1} = P_{z2}$ = 18000 Kp (Tables 2 and 3). This means that it is about 18% smaller than the shock force P_z = 22000 Kp assumed for the design case "Two-point horizontal landing with 25% drag" assumed to occur at w_s = 4 m/sec and G = 21800 Kp.

The largest shock absorbing strut stroke determined from 22 vertical landings and which of course occurs during the second landing shock is f_2 = 337 mm (Table 3) and is therefore 19% smaller than the maximum possible stroke of 416 mm.

The shock forces P_y are greater for most of the 23 measured vertical landings than for the first landing shock (Tables 2 and 3), just like the forces P_z. /29

However, their relative magnitudes nor their time of occurrence are usually not related to those of the P_z forces.

The curves showing the frequency distributions of the maximum absolute values of the shock factors e_{y1} during the first landing shock in Figure 10 and those of e_{y2} for the second landing shock in Figure 11 clarify the harder frequency distribution of P_y during the second landing shock.

The largest shock force P_y on one undercarriage side is P_{y1} = 4000 kp for the first landing shock (Table 2) and P_{y2} = 3800 kp for the second landing shock (Table 3). The largest p_y forces do not coincide with the largest P_z forces (which can be explained by the fact that the magnitude of P_y depends primarily on the side motion of the aircraft (sideslip landing).

In the design assumptions for the DO 31, we assumed according to the helicopter specifications MIL-S-8698 and for a vertical landing with a side wind of w_s = 3 m/sec and S/G - 2/3, a side force of $P_y = 0.5 \cdot P_z$. With a design landing weight of G = 21 800kp, we have P_z = 19 400 kp and therefore P_y or $e_y = 2 \cdot P_y/G$ = 0.9, respectively, per main undercarriage side.

Since the magnitude of the P_y forces probably depends greatly on the operational and landing characteristics (for

example, side wind and airport roughnesses), the results obtained from the 23 vertical landings of the NASA testing program are not sufficient for generally valid statements on permissible side loads. This is especially true if we consider the especially favorable environmental conditions (good weather conditions, selected landing sites).

The P_x forces could only be determined on the right undercarriage side during the 23 measured vertical landings, with the exception of one landing (experiment No. 220), because the corresponding strain gauge bridge failed. As expected, they are smaller because of the small horizontal landing velocity, compared with the P_x forces which are decisive for the design. These forces occur for the load cases (braking), "vertical landing spin up" and "two-point landing fuselage down springback" for conventional landings. /30

This means that the P_x forces determined from these measurements are very restricted and do not suffice for a general statement regarding the expected P_x forces during vertical landings.

6. CONCLUSIONS FROM THE RESULTS OF THE LANDING MEASUREMENTS

Considering certain restrictions such as the relatively low number of measured landings and the fact that the testing was performed by experienced test pilots with very extensive /31 safety measures, we can nevertheless draw some conclusions for the design of VTOL aircraft. We can derive some interactions to be used in the conception of new landing techniques and methods. The configuration and design of the engine installation of the Do 31 represents another factor which limits the generality of our conclusions. Nevertheless, we believe that the basic conclusions drawn should be valid for other engine

configurations.

The vertical landings performed by the Do 31 were manually controlled according to the pilot's vision during the last phase of descent (from a height of 5-10 m). The test results show an accumulation of the measured sinking velocities at a value of 2 m/sec with a maximum value up to 3.4 m/sec. Sinking velocities below 1 m/sec do not occur at all. Compared with conventional landings, vertical landings are in general much harder according to the sinking velocities (Figures 14 and 18).

Another result of the test is that there is a rebound of the aircraft after the first touchdown which results in a second shock with considerably higher shock loads. It is included in the collection of sinking velocities by introducing a fictitious sinking velocity. This then leads to an even harder collection of sinking velocities (Figure 15). Considering the design sinking velocity of 4 m/sec for the Do 31, this means that there is a smaller safety margin compared with conventional applications. This is especially true considering the much more unfavorable fatigue loads caused by the landing shock forces.

Based on the present results we may conclude the following: /32
If the minimum requirements for landing sinking velocity are to be applied for future developments as specified in the specifications "FAR.XX" of the FAA or the "Provisional Airworthiness Requirements for Civil PL-Aircraft" of the ARB, this can only be done under the assumption that another landing technique is used. For example, a sinking velocity control could be used which would assure that the sinking velocities specified in the design documents would not be exceeded during operation. Such a landing technique would be especially advantageous for civilian passenger traffic, especially from the point of view of passenger comfort. These requirements should be easy to

comply with because a sinking velocity control system is necessary any way in order to control the vertical landing.

In addition, a positive influence on the rebound after touchdown can be obtained by optimizing the undercarriage shock absorber system in the direction of vertical landings. Also the shock loads could be reduced in this way. This would also be advantageous for the design of a control system.

We cannot give any statistical information on the measured side loads P_y because of the small number of measured landings. Compared with the vertical loads, the measured side loads lie within the design limits. In this connection it is interesting to note that according to information obtained from the pilots, the side motions of the aircraft are easy to control during hovering flight. Therefore, we do not expect any special difficulties, at least for flight over flat land.

Civilian Regulations: /34

USA:

Federal Aviation Regulations (FAR)

PART 23: Valid for small aircraft
PART 25: Valid for commercial aircraft
PART 27: Valid for small helicopters
PART 29: Valid for small commercial rotary aircraft
PART XX: Design of VSTOL aircraft

Great Britain:

British Civil Airworthiness Requirements (BCAR)
Section D: Airplanes: valid for aircraft in general

Provisional Airworthiness Requirements for Civil Powered-Lift Aircraft: design for VSTOL aircraft

Military Specifications:

USA:

Military Specification MIL-A-008862A
"Airplane Strenght and Rigidity, Landing and Ground Handling Loads"

Military Specification MIL-A-008866A
"Airplane Strength and Rigidity Reliability Requirements, Repeated Loads and Fatigue"

Military Specification MIL-S-8698
"Structural Design Requirements, Helicopters"

TABLE I. LANDING STATE VARIABLES

/35

Exp. No.	G [kp]	U [ku]	Θ (deg)	ϕ (deg)	w_{s_1} [m/sec]	w_{s_2} [m/sec]	$\bar{w}_{s_1}$ [m/sec]
220	18 245	6	7	0,5	2,3	1,3	1,9
222	18 325	20	4	0	3,0	1,4	2,6
223	17 805	20	7	2	2,7	1,1	2,7
225	17 927	2	8	3	1,9	1,3	2,2
226	18 230	22	6	– 1,5	2,4	1,4	2,6
227	18 270	9	9	1	1,9	0,8	1,9
228	17 605	16	8	0,5	3,4	1,2	2,5
229	18 320	16	5	– 1,5	2,6	1,5	3,0
231	17 515	25	6	– 0,5	3,1	1,4	3,2
232	18 483	25	6	1	2,9	1,3	2,5
233	18 275	19	3	1	2,5	1,6	2,9
234	18 708	13	8	2	2,7	1,2	2,0
235	18 936	10	13	3,5	1,9	1,4	2,5
236	18 700	5	7	0,5	2,2	1,5	2,6
237	18 137	4	6	– 1	2,1	1,8	2,3
238 b	18 930	3	8	– 2,5	1,6	1,4	2,3
239	18 400	20	6	1,6	2,3	1,2	2,8
240	18 568	21	8	– 4	1,9	2,1	3,3
241	18 132	25	8	– 1,5	1,9	1,4	2,6
243	18 545	30	6	2	2,4	2,3	3,4
244	18 700	12	7	1	1,7	1,5	2,6
247	18 356	15	5	2,5	2,3	1,6	3,1
248	18 833	12	5	2,5	2,2	1,3	2,4

TABLE II. UNDERCARRIAGE SHOCK FORCES, SHOCK FORCE FACTORS AND SHOCK ABSORBER STRUT STROKES FOR FIRST LANDING SHOCK

/36

Exp. No.	P_{x_1} [kp]	P_{y_1} [kp]	P_{z_1} [kp]	e_{x_1}	e_{y_1}	e_{z_1}	f_1 [mm]
	Left Right	Left Right	Left Right	Left Right	Left Right	Left Right	Left Right
220	– 560 – 460	740 1 390	9 500 11 500	– 0,091 – 0,05	0,091 0,152	1,04 1,26	241 269
222	– 370	– 700 720	14 600 14 000	– 0,04	– 0,076 0,079	1,59 1,53	305 304
223	– – 560	520 1 070	11 500 13 500	– – 0,063	0,059 0,12	1,29 1,52	260 305
225	– – 1 110	– 1 030 3 080	6 200 10 400	– – 0,125	– 0,115 0,345	0,69 1,16	139 217
226	– – 2 040	– 2 070 – 2 060	10 000 11 500	– – 0,224	– 0,227 – 0,226	1,1 1,26	223 271
227	– – 1 300	– 650 680	9 500 7 500	– – 0,142	– 0,071 0,074	1,04 0,82	239 173
228	– – 2 590	2 010 2 240	18 000 15 000	– – 0,294	0,228 0,255	2,04 1,71	319 313
229	– – 1 670	1 100 1 640	12 000 12 000	– – 0,182	0,12 0,179	1,31 1,31	200 200
231	– – 1 850	2 080 2 360	14 600 14 800	– – 0,211	0,238 0,27	1,69 1,69	313 308
232	– – 2 590	2 000 1 890	14 000 13 600	– – 0,28	0,216 0,203	1,51 1,47	301 288
233	– – 1 480	1 730 1 960	11 400 11 600	– – 0,162	0,19 0,215	1,25 1,27	270 273
234	– – 2 040	850 1 650	12 600 13 000	– – 0,218	0,091 0,177	1,35 1,39	282 287
235	– – 2 400	370 1 940	7 800 9 200	– – 0,254	0,04 0,205	0,82 0,97	197 226
236	– – 1 480	– 2 900 – 1 880	9 000 11 500	– – 0,158	– 0,31 – 0,2	0,96 1,12	– –
237	– – 930	– 570 – 1 930	5 800 9 200	– – 0,102	– 0,063 – 0,213	1,09 1,02	248 241
238 b	– 740	– 1 370 – 2 350	8 000 5 000	– – 0,078	– 0,145 – 0,238	0,85 0,53	198 114
239	– 2 220	600 960	9 800 11 200	– 0,24	0,065 0,105	1,07 1,2	235 262
240	– – 930	– 3 080 300	9 500 6 000	– – 0,1	– 0,332 0,032	1,02 0,65	218 161
241	– – 2 410	1 270 300	7 200 9 200	– – 0,256	0,14 0,033	0,79 1,02	165 227
243	– – 930	2 320 3 290	10 800 11 600	– – 0,1	0,25 0,3	1,17 1,25	266 261
244	– – 1 110	920 620	8 000 5 800	– – 0,12	0,099 0,066	0,86 0,62	219 155
247	– 1 200	2 040 4 000	10 000 11 000	– 0,13	0,222 0,438	1,09 1,2	223 240
248	– – 370	1 210 1 420	9 800 10 500	– – 0,04	0,129 0,151	1,04 1,12	248 265

TABLE III. UNDERCARRIAGE SHOCK FORCES, SHOCK FORCE FACTORS AND SHOCK ABSORBING STRUT STROKES FOR SECOND LANDING SHOCK

/37

Exp. No.	P_{x_2} [kp] Left / Right	P_{y_2} [kp] Left / Right	P_{z_2} [kp] Left / Right	e_{x_2} Left / Right	e_{y_2} Left / Right	e_{z_2} Left / Right	f_{o_2} [mm] Left / Right	f_2 [mm] Left / Right
220	1 390 1 390	- 940 - 2 300	6 000 9 600	0,152 0,152	- 0,103 0,252	0,66 1,05	115 155	166 254
222	- - 370	- 2 560 - 2 840	11 000 13 000	- - 0,039	- 0,28 - 0,31	1,2 1,43	120 200	277 297
223	- 1 950	3 050 3 800	13 400 12 000	- 0,219	0,343 0,427	1,51 1,35	117 134	295 249
225	- 1 200	3 800 2 870	11 000 8 400	- 0,134	0,424 0,32	1,23 0,94	102 107	265 246
226	- 650	- 1 720 - 2 600	11 400 12 400	- 0,071	- 0,189 - 0,285	1,25 1,36	62 132	277 290
227	- 370	880 - 910	9 000 8 000	- 0,039	0,096 - 0,099	0,99 0,88	100 107	227 230
228	- 740	- 2 860 - 2 960	10 000 12 200	- 0,084	- 0,325 - 0,336	1,14 1,39	152 187	255 301
229	- - 370	980 - 840	14 000 15 000	- - 0,04	0,107 - 0,092	1,53 1,64	126 120	304 320
231	- - 740	- 3 180 - 2 350	12 200 16 800	- - 0,085	- 0,363 - 0,268	1,39 1,92	152 172	285 337
232	- 370	- 1 850 - 1 990	11 000 12 600	- 0,01	- 0,2 - 0,215	1,19 1,36	179 157	277 290
233	- - 740	800 - 900	13 000 14 000	- - 0,081	0,088 - 0,099	1,42 1,53	135 124	297 312
234	- 560	- 1 000 1 640	9 200 9 000	- 0,06	- 0,107 0,175	0,98 0,96	86 63	248 248
235	- - 2 600	2 960 1 110	13 000 10 200	- - 0,275	0,3 0,117	1,38 1,08	95 94	295 255
236	- - 190	2 060 1 600	14 600 9 600	- - 0,02	0,22 0,17	1,56 1,03	- -	- -
237	- - 190	- 2 070 - 2 580	9 000 11 200	- - 0,02	- 0,228 - 0,285	0,99 1,24	80 98	240 272
238 b	- - 650	- 3 690 - 1 690	7 200 12 800	- - 0,07	- 0,39 - 0,18	0,76 1,35	84 57	223 242
239	- 190	- 820 740	13 000 13 200	- 0,02	- 0,09 0,08	1,41 1,44	103 139	295 301
240	- 1 200	2 690 - 2 850	16 000 17 000	- 0,13	0,29 - 0,31	1,73 1,83	0 0	304 329
241	- - 560	- 2 050 2 930	12 400 11 200	- - 0,062	- 0,226 0,323	1,37 1,24	0 82	280 268
243	- 1 200	1 370 1 030	16 000 18 000	- 0,13	0,148 0,111	1,73 1,94	87 78	319 322
244	- 1 110	- 2 470 - 2 300	13 500 11 000	- 0,12	- 0,264 - 0,246	1,44 1,18	72 0	298 281
247	- - 460	1 090 700	13 800 16 000	- - 0,05	0,119 0,076	1,5 1,74	68 70	306 321
248	- - 740	440 960	9 800 12 000	- - 0,079	0,047 0,102	1,04 1,28	104 120	263 285

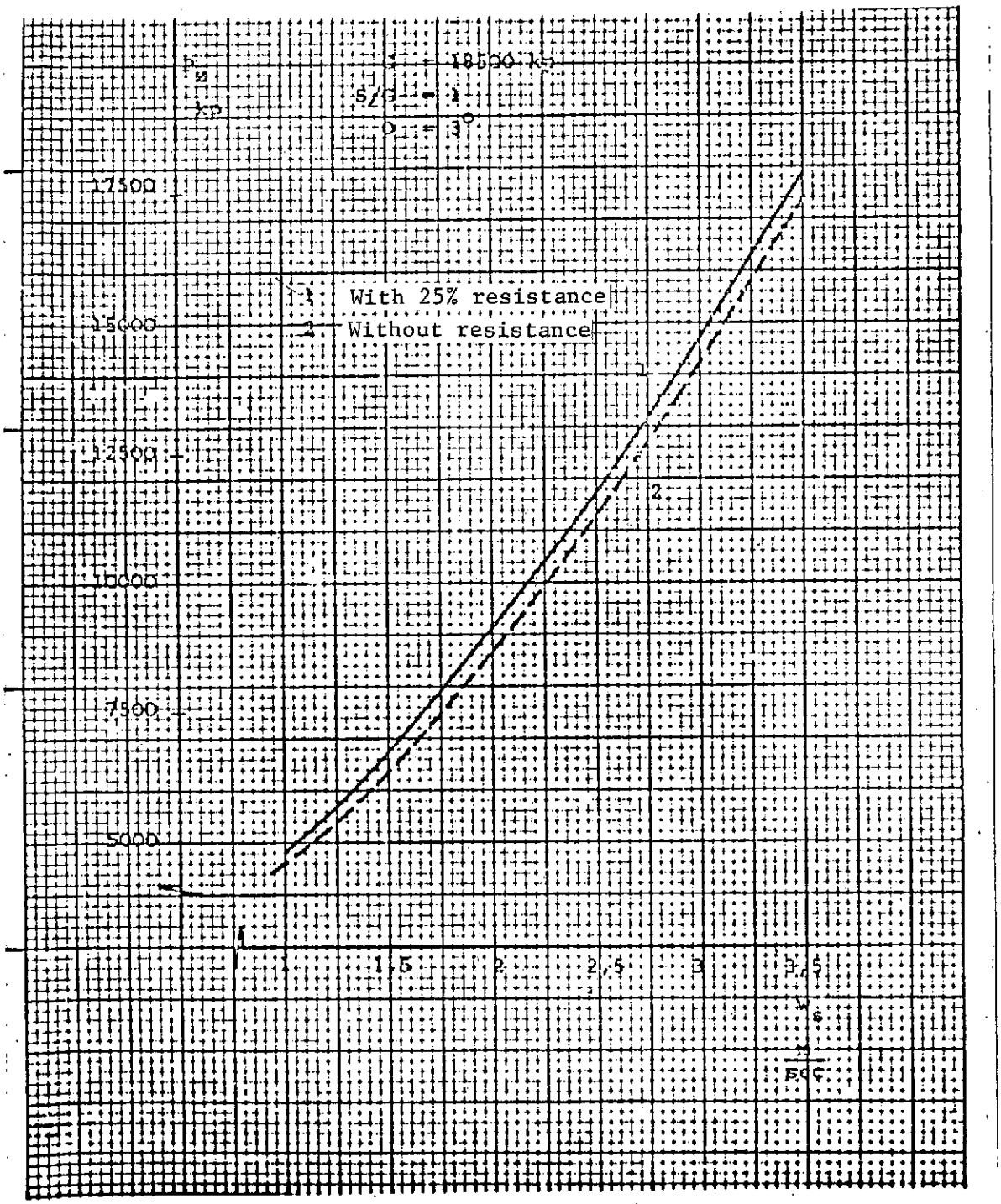

Figure 1. Shock force P_z as a function of sinking velocity w_s (from motion calculations of the landing shock process) for Do 31-E3

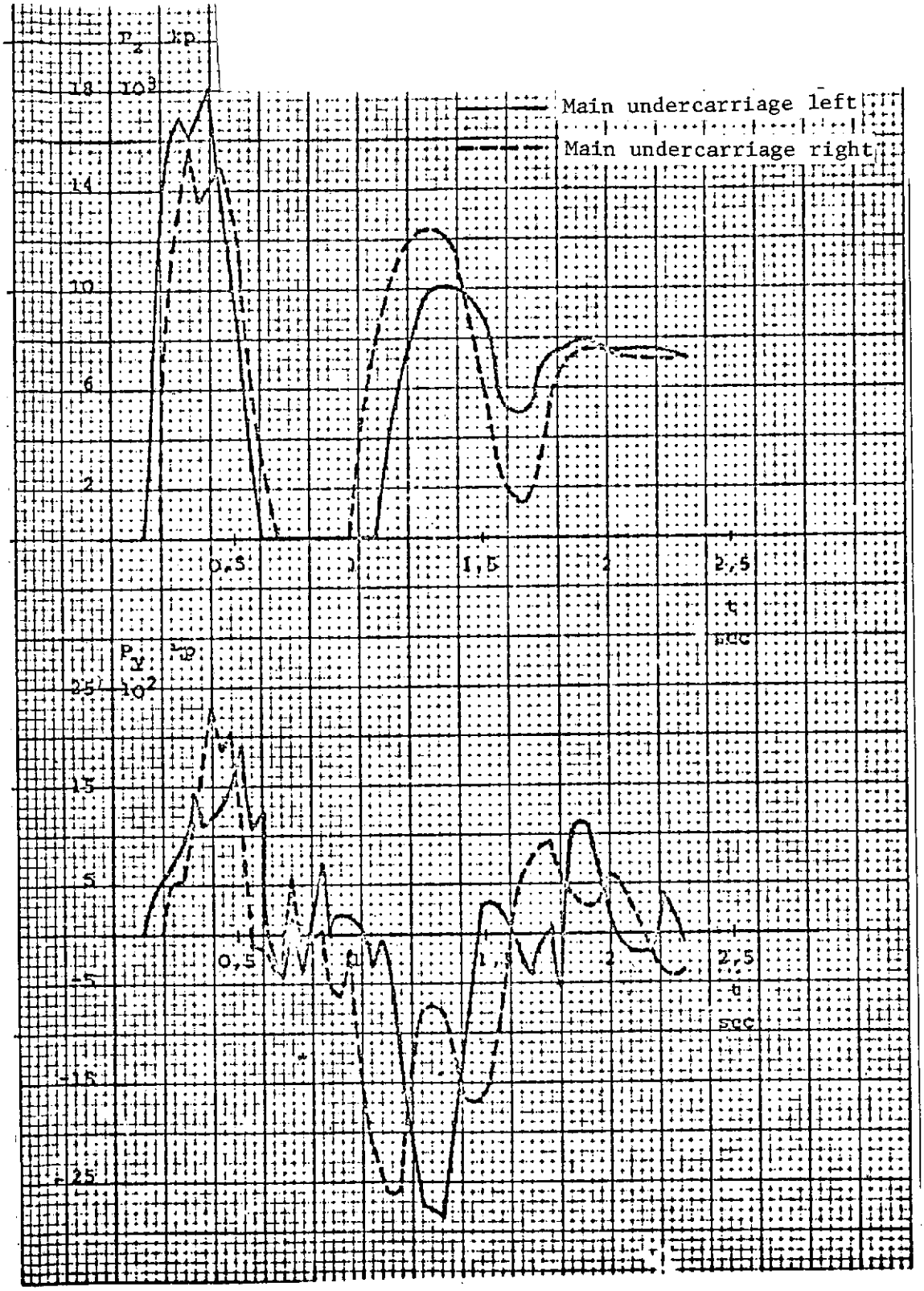

Figure 2. Measured time variation of the landing shock forces P_z and P_y from Experiment No. 228

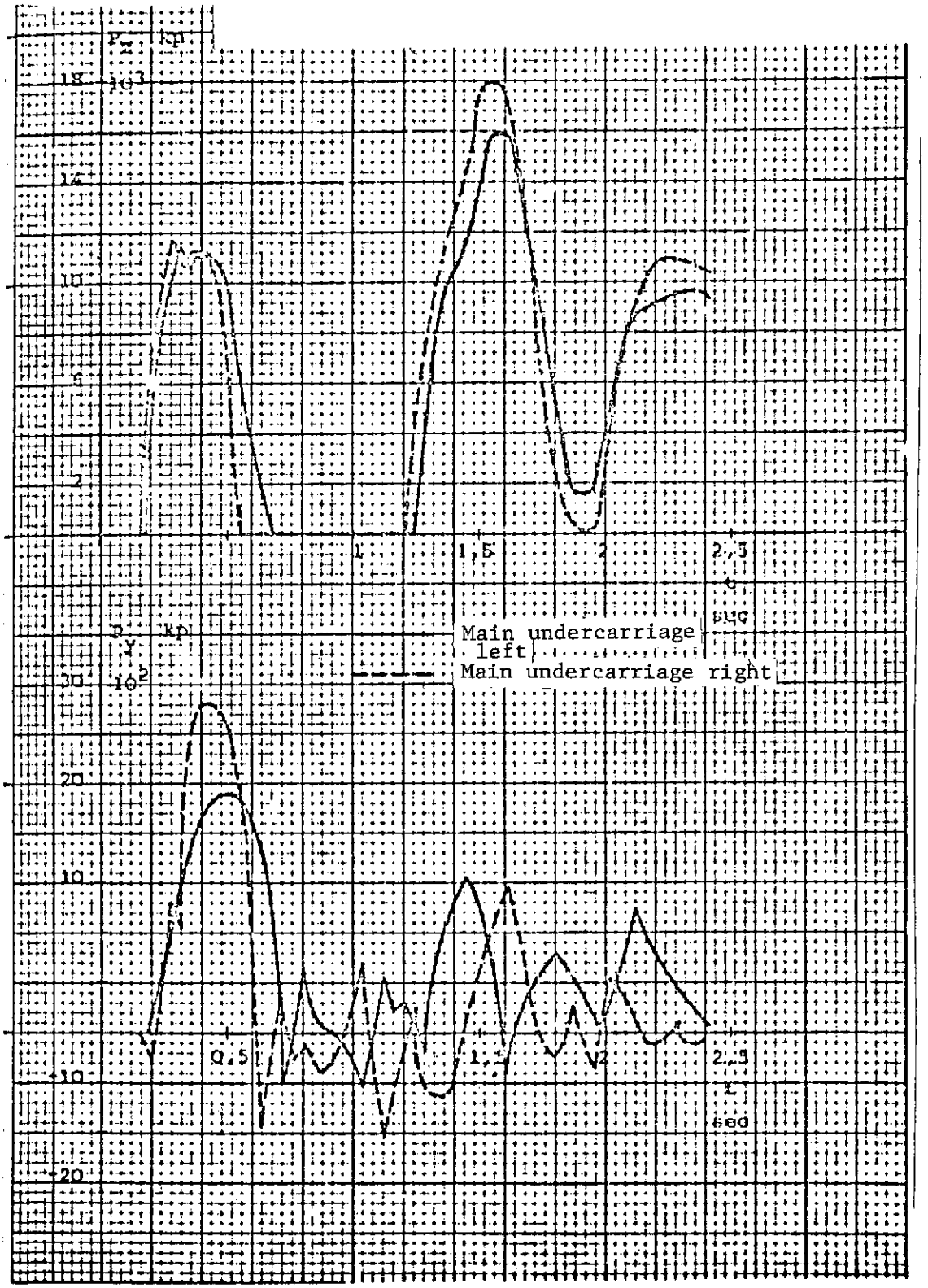

Figure 3. Measured time variation of the landing shock forces P_z and P_y from Experiment No. 213

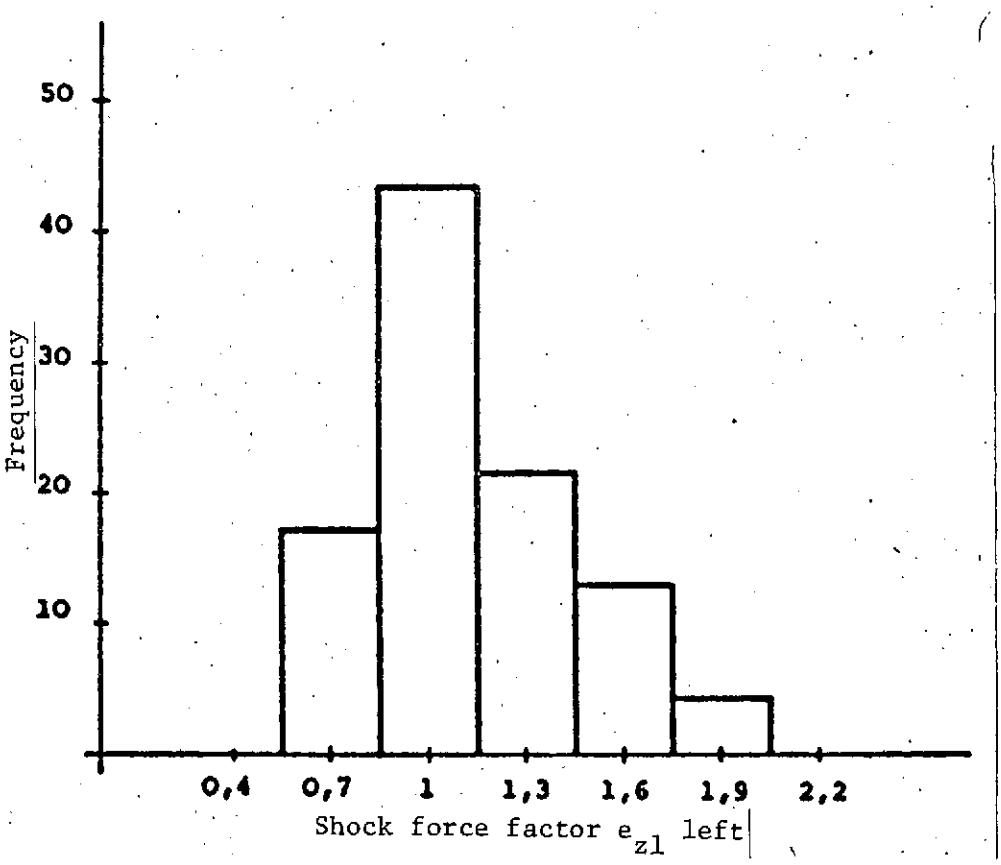

Figure 4. Frequency distribution of the shock force factors e_{z1} left from 23 vertical landings

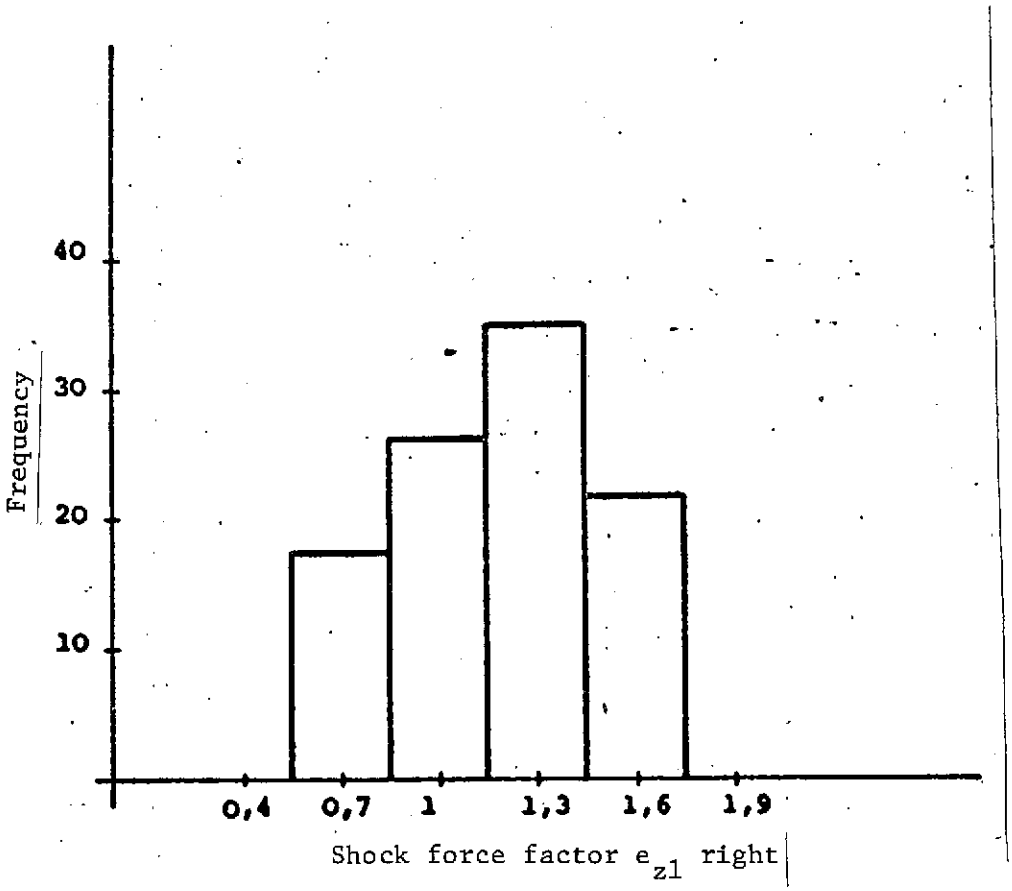

Figure 5. Frequency distribution of the shock force factor e_{z1} right from 23 vertical landings

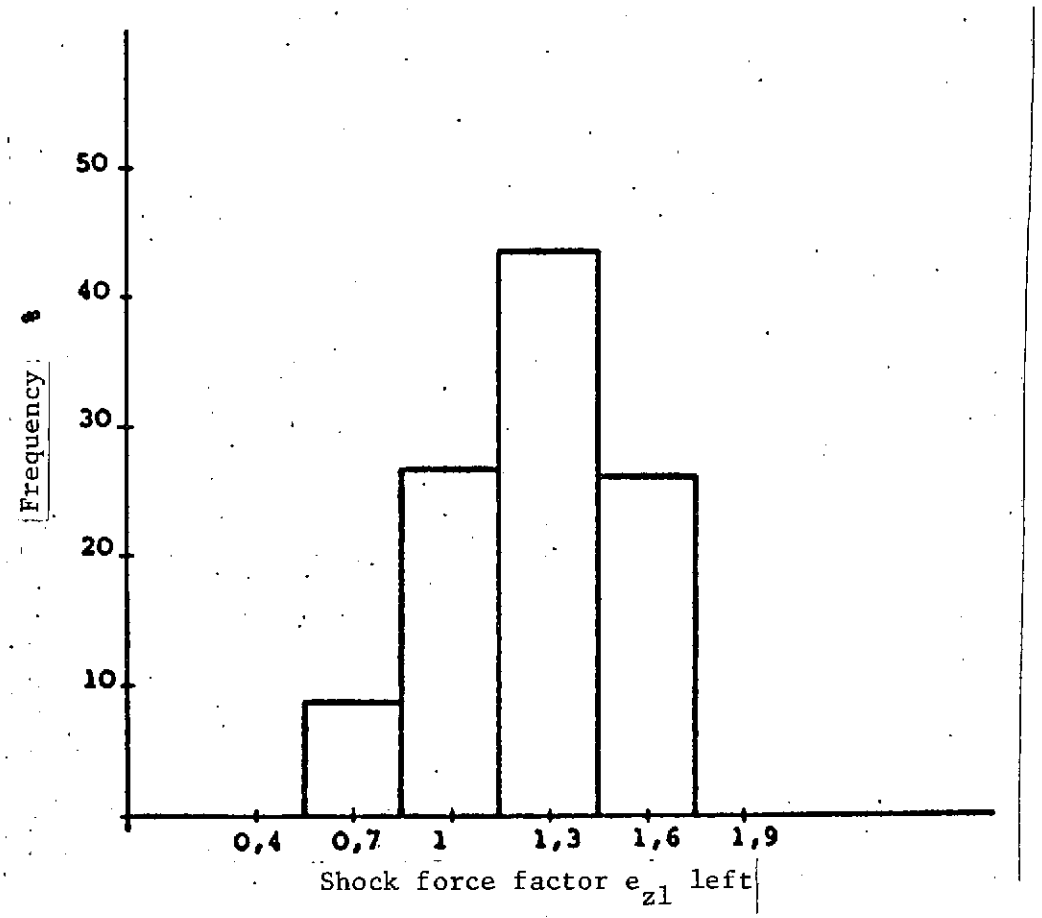

Figure 6. Frequency distribution of the shock force factor e_{z1} left from 23 vertical landings

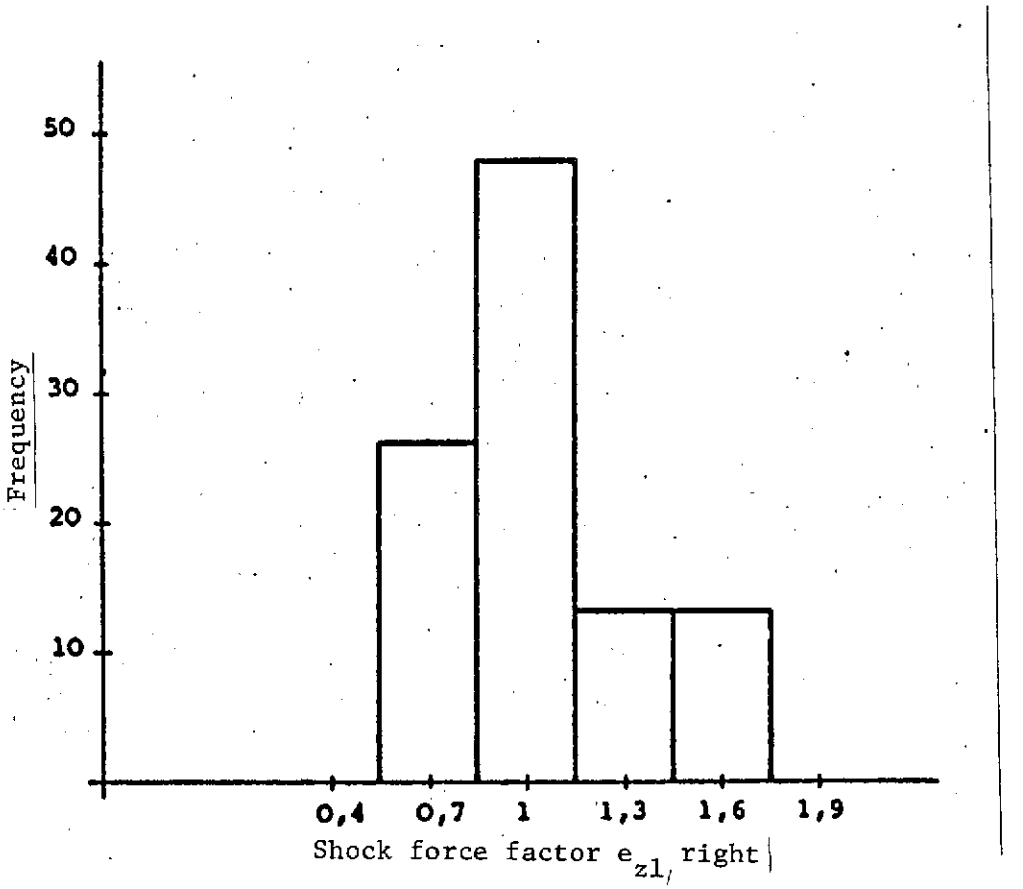

Figure 7. Frequency distribution of the shock force factor e_{z1} right from 23 vertical landings

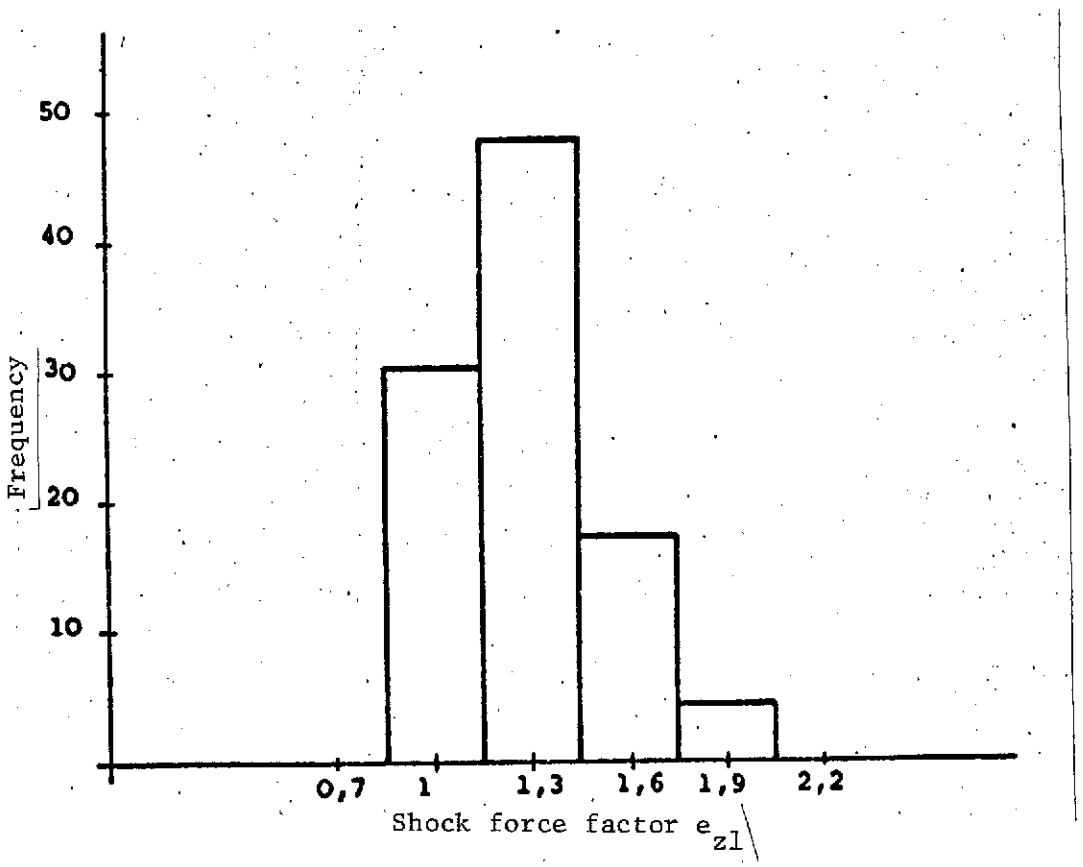

Figure 8. Frequency distribution of the largest shock force factors e_{zl} left or right from 23 vertical landings

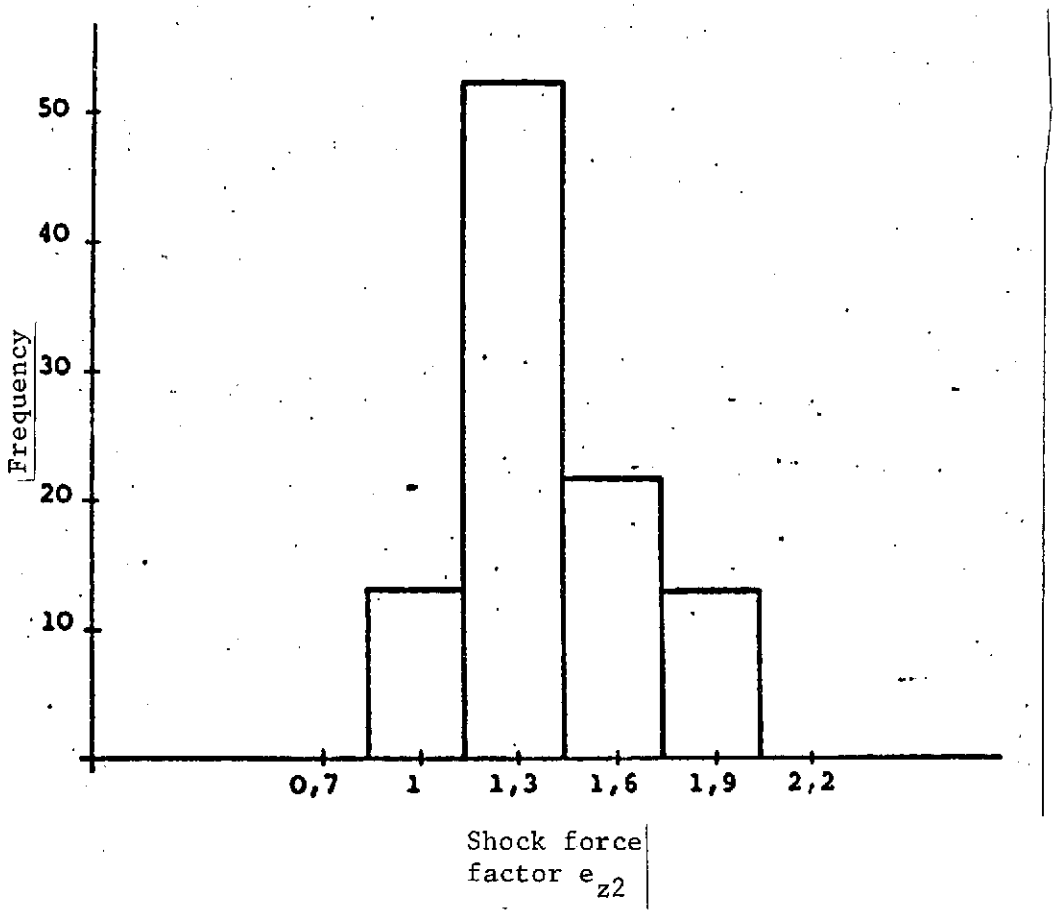

Figure 9. Frequency distribution of the largest shock force factors e_{z2} left or right from 23 vertical landings

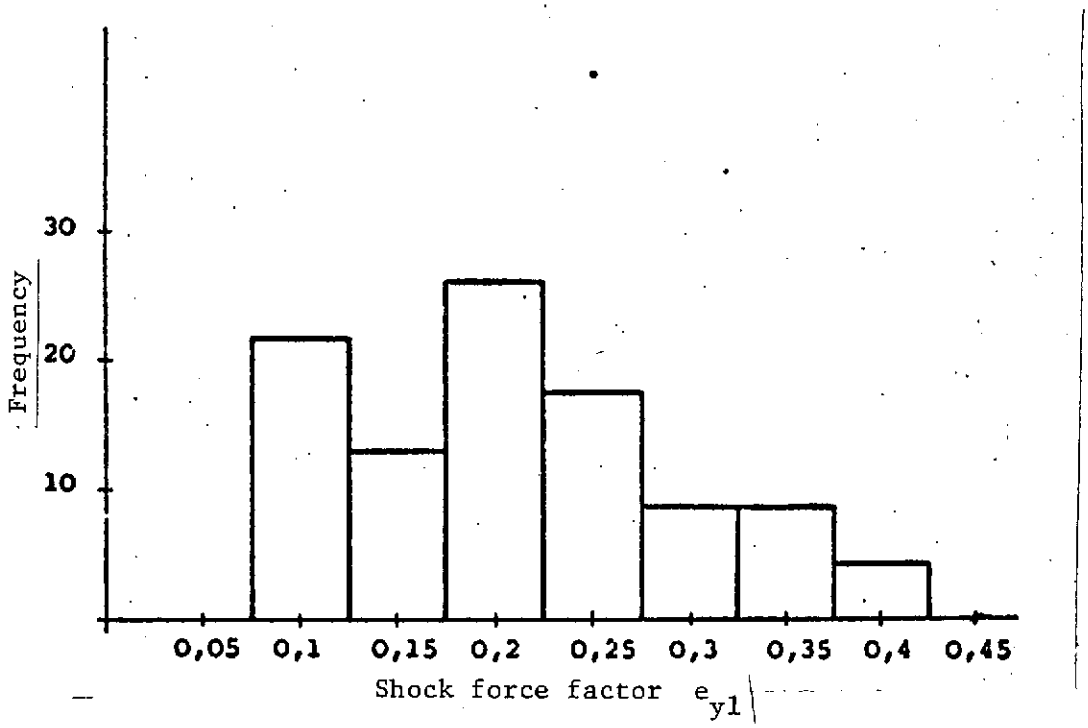

Figure 10. Frequency distribution of the largest shock force factors e_{y1} left or right from 23 vertical landings

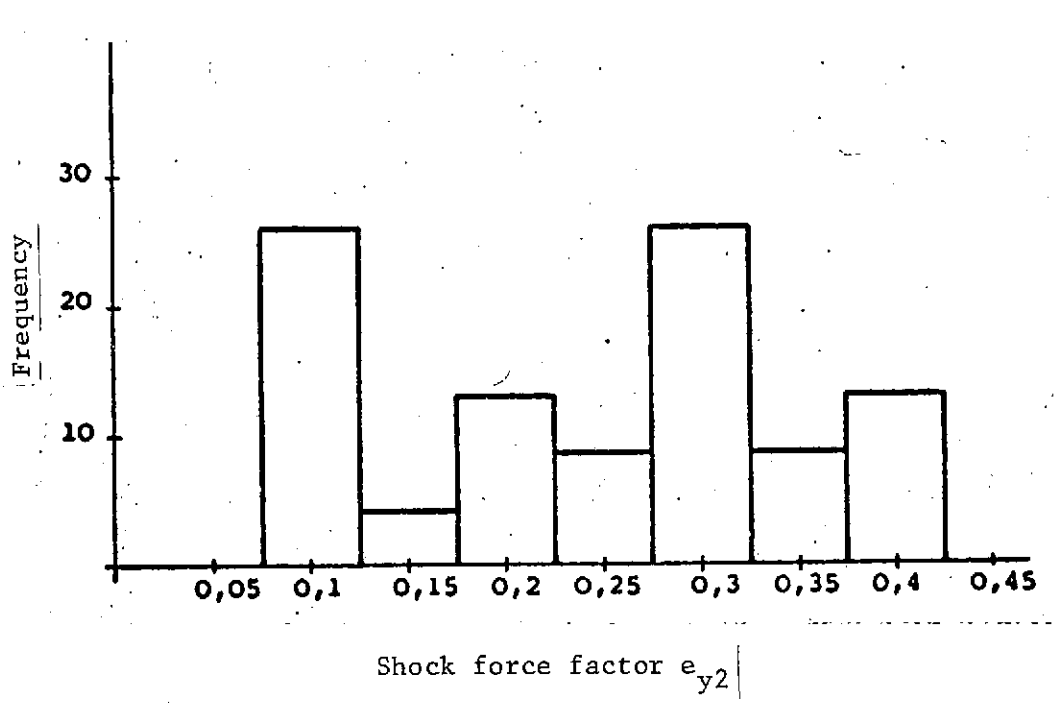

Figure 11. Frequency distribution of the largest shock force factors e_{y2} left or right from 23 vertical landings

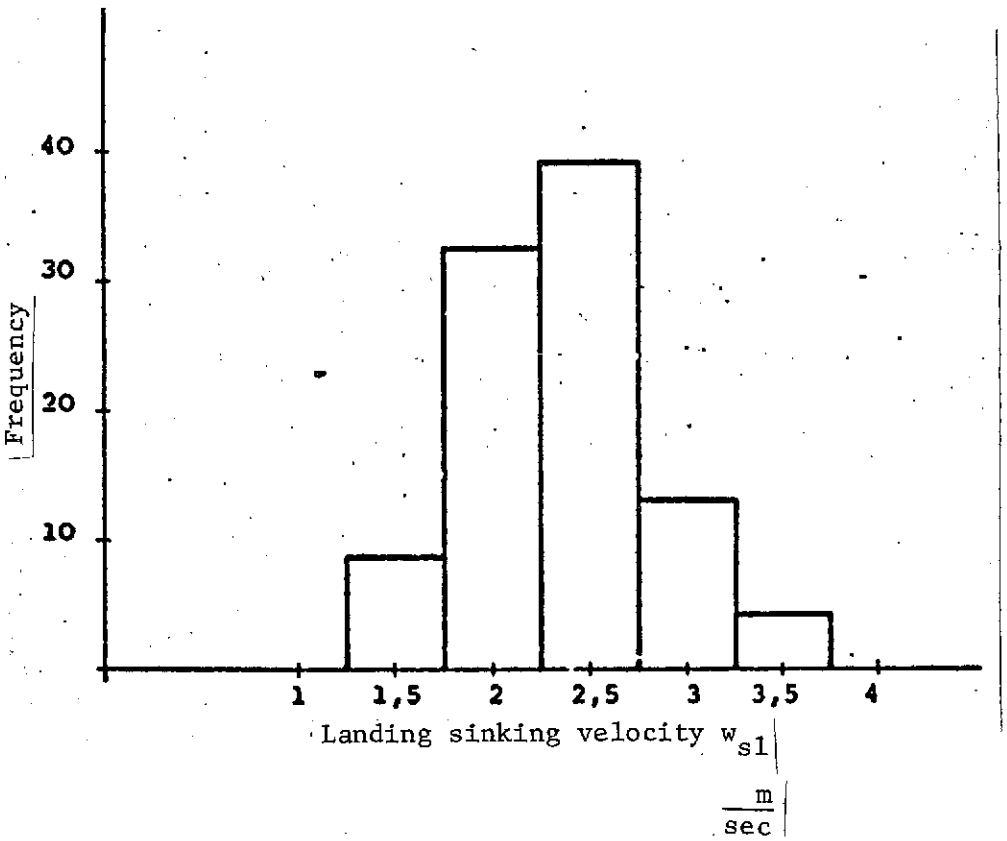

Figure 12. Frequency distribution of the landing sinking velocity w_{sl} from 23 vertical landings during the NASA test program

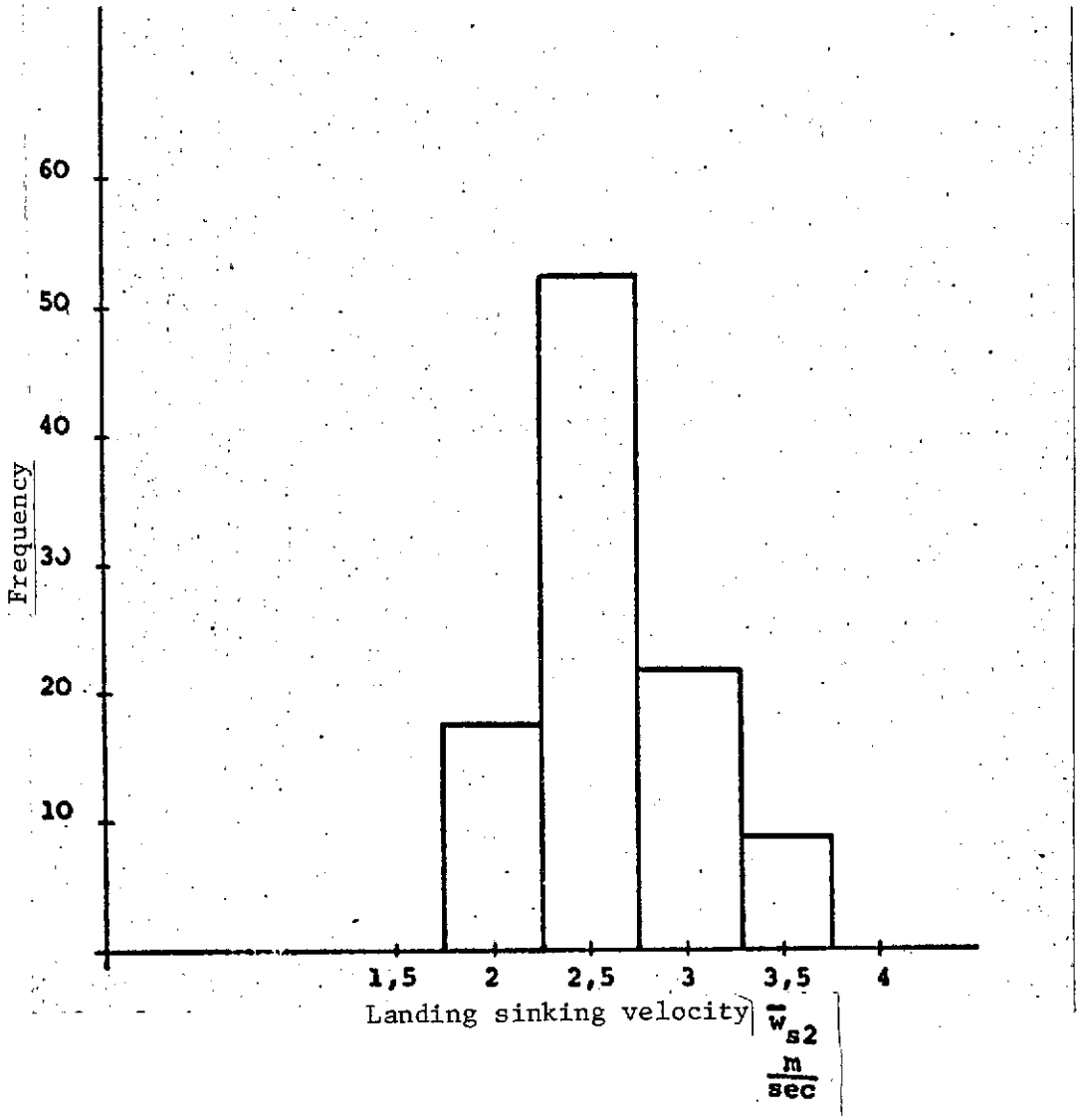

Figure 13. Frequency distribution of the fictitious landing sinking velocity $\bar{w}_{s2}$ from 23 vertical landings during the NASA test program

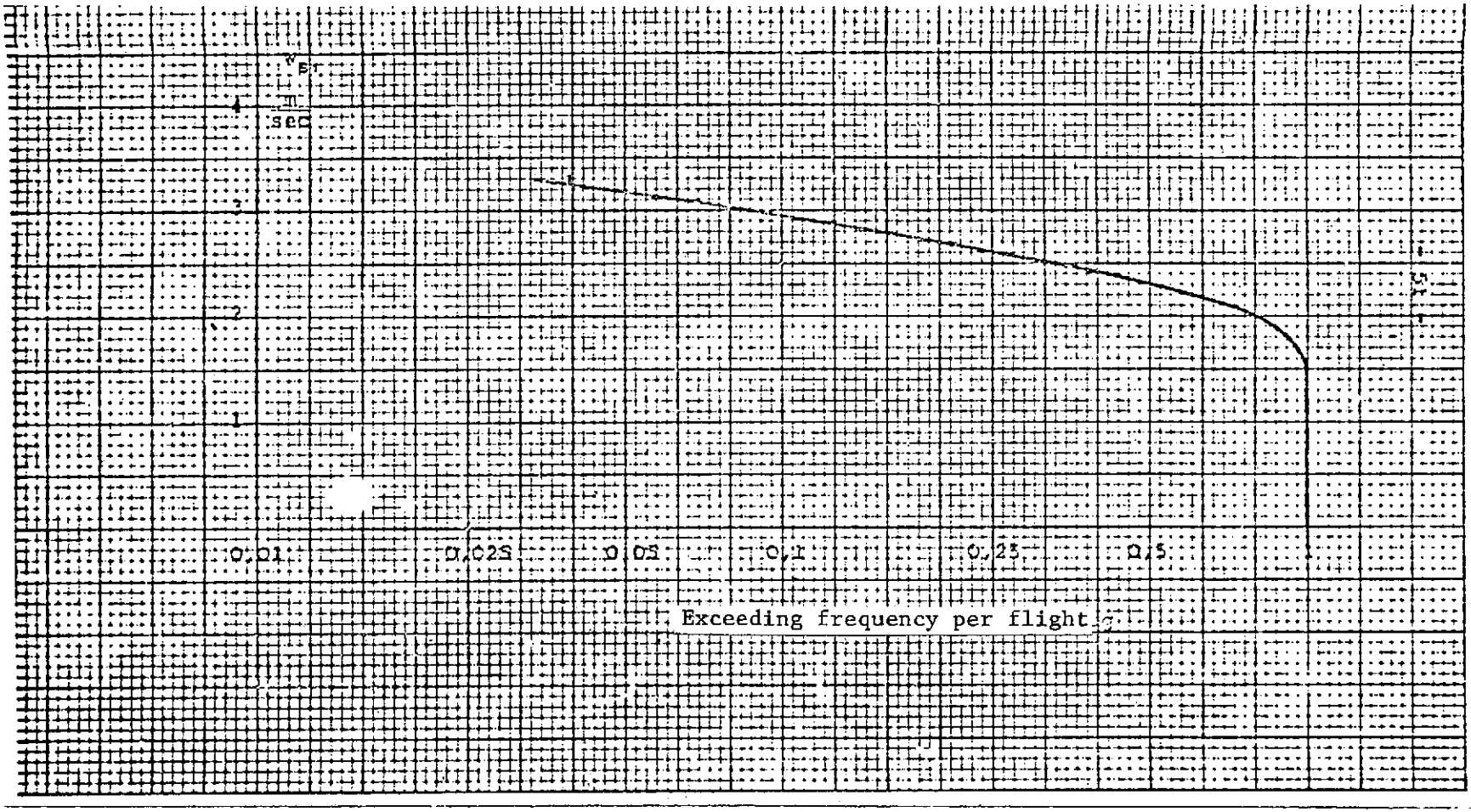

Figure 14. Exceeding frequency of the landing sinking velocity w_{sl} per flight from 23 vertical landings during the NASA test program

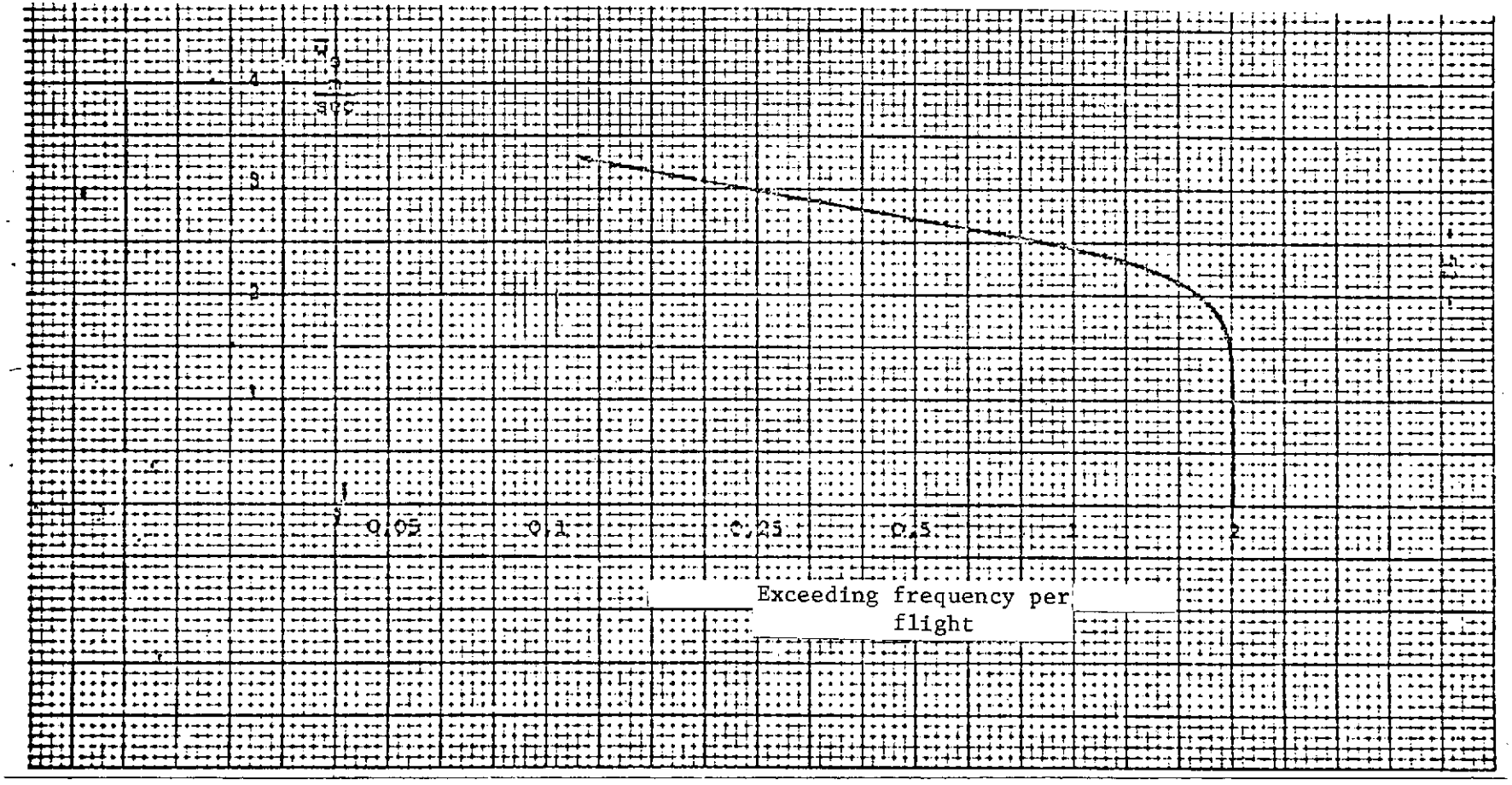

Figure 15. Exceeding frequency of the fictitious landing sinking velocity $\bar{w}_s$ per flight including the second landing shock from 23 vertical landings during the NASA test program

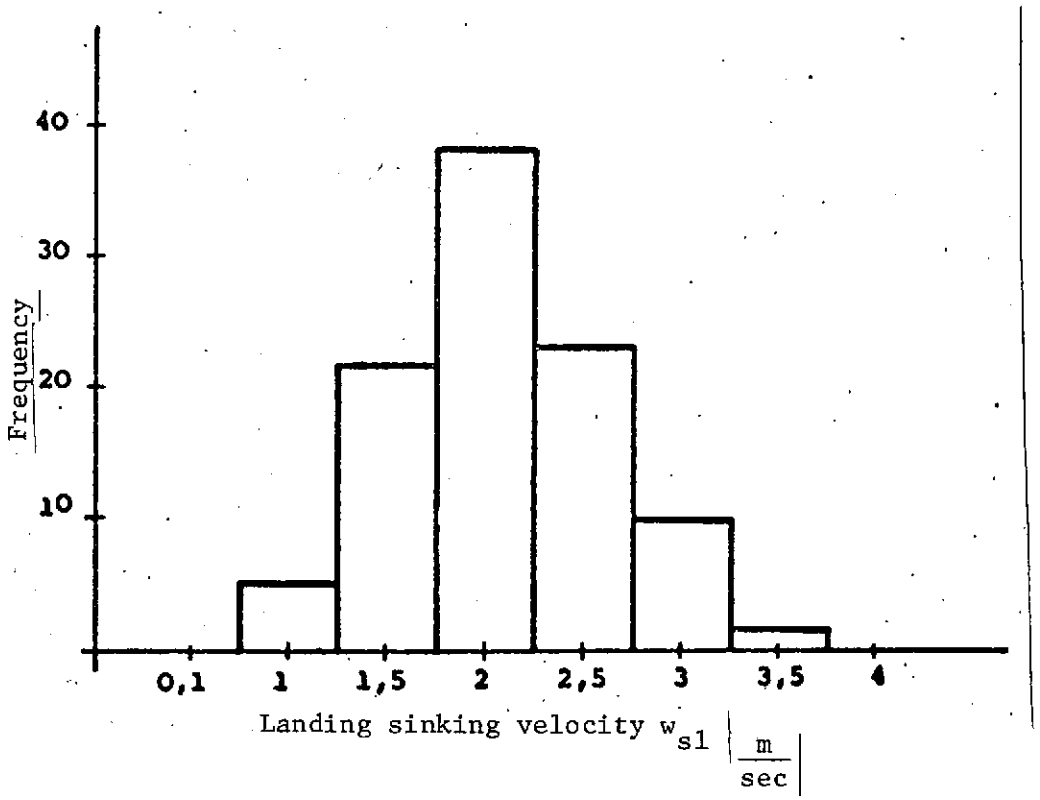

Figure 16. Frequency distribution of the landing sinking velocity w_{s1} according to [4] from 60 vertical landings for basic test program

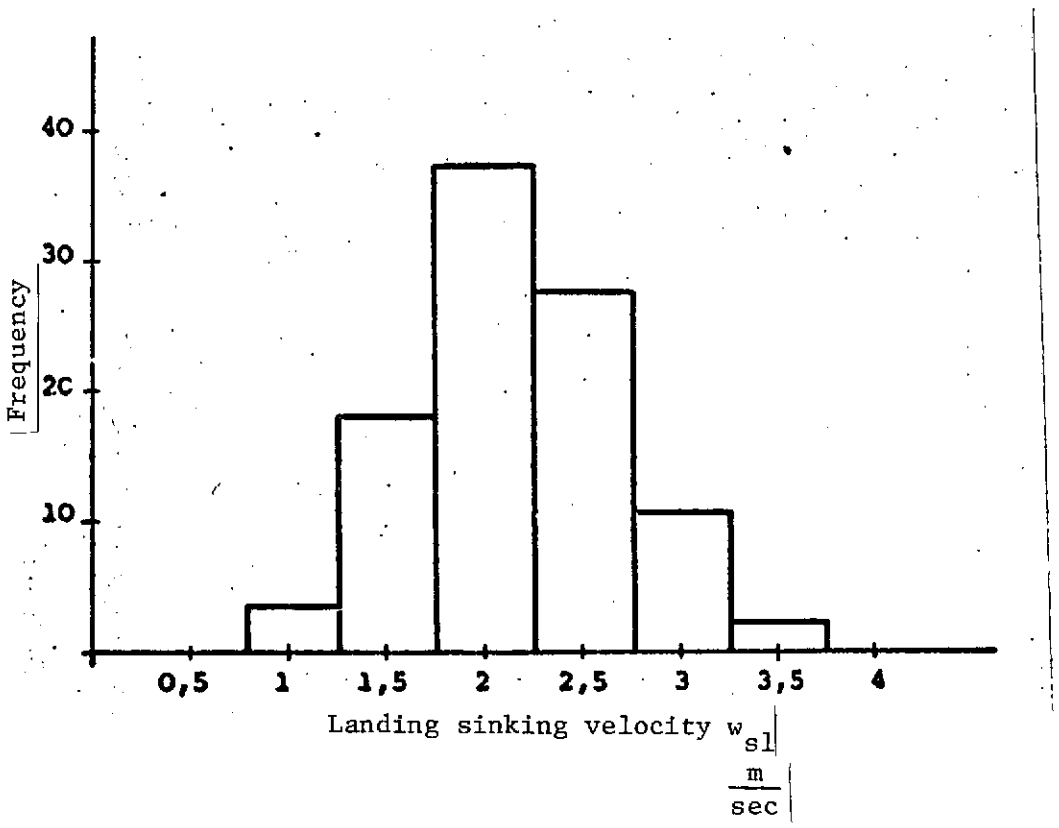

Figure 17. Frequency distribution of the landing sinking velocity w_{sl} from 83 vertical landings (23 landings during NASA test program and 60 landings for basic training program)

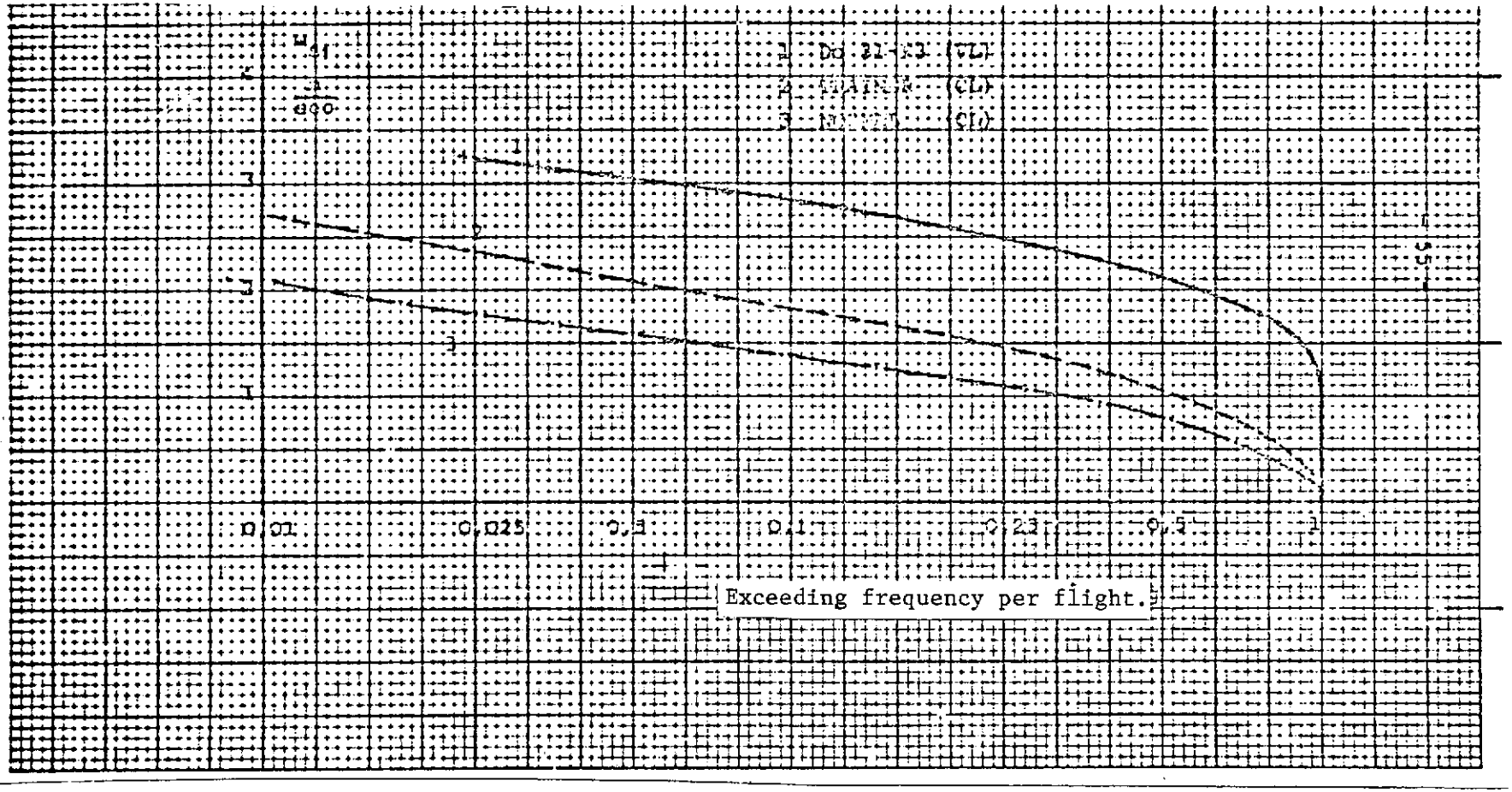

Figure 18. Exceeding frequency of the landing sinking velocity (8) per flight (*)

* Translator's note: Illegible in foreign text.

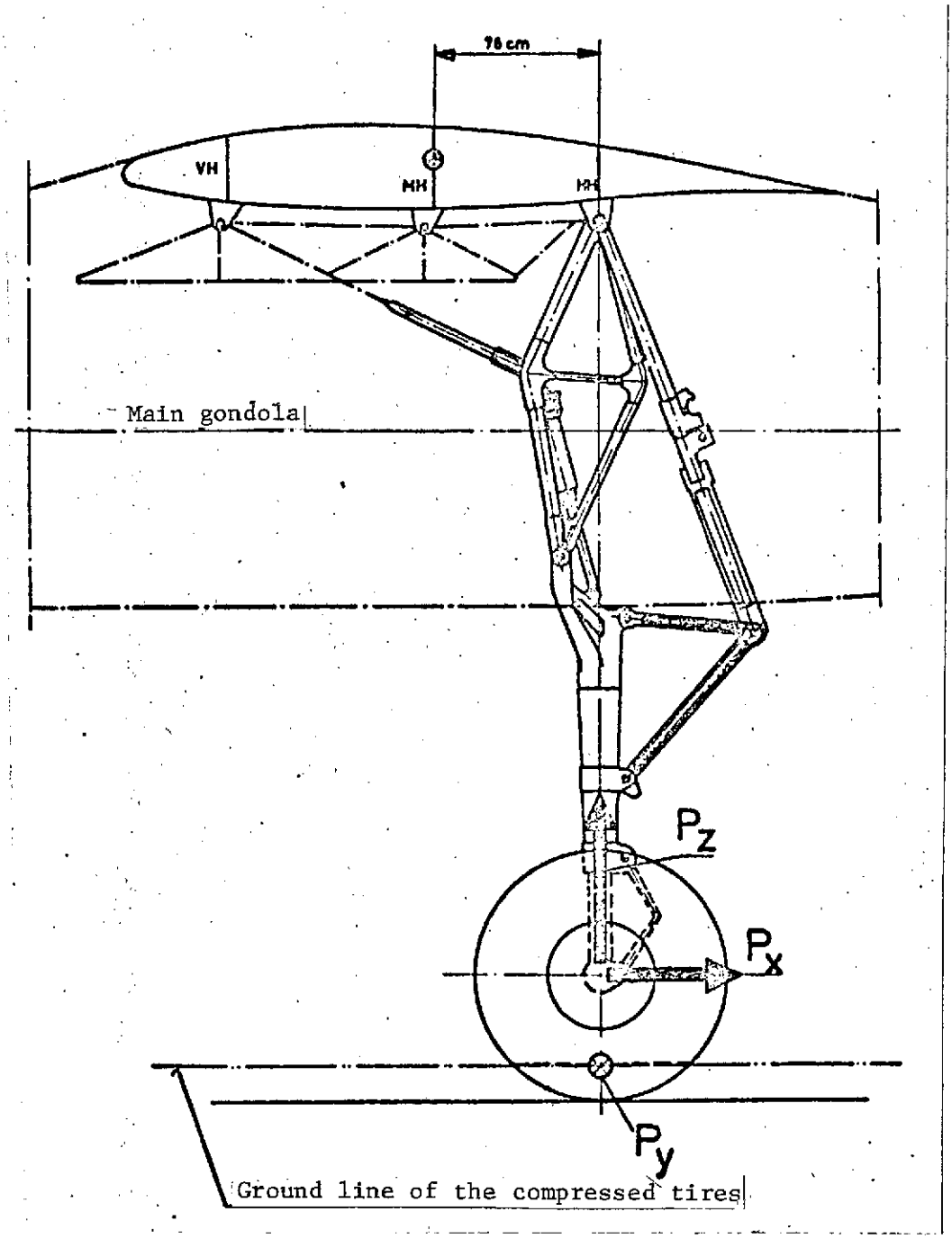

Figure 19. Arrangement and design of main undercarriage

Measurement points on the main undercarriage of the Do 31 E1

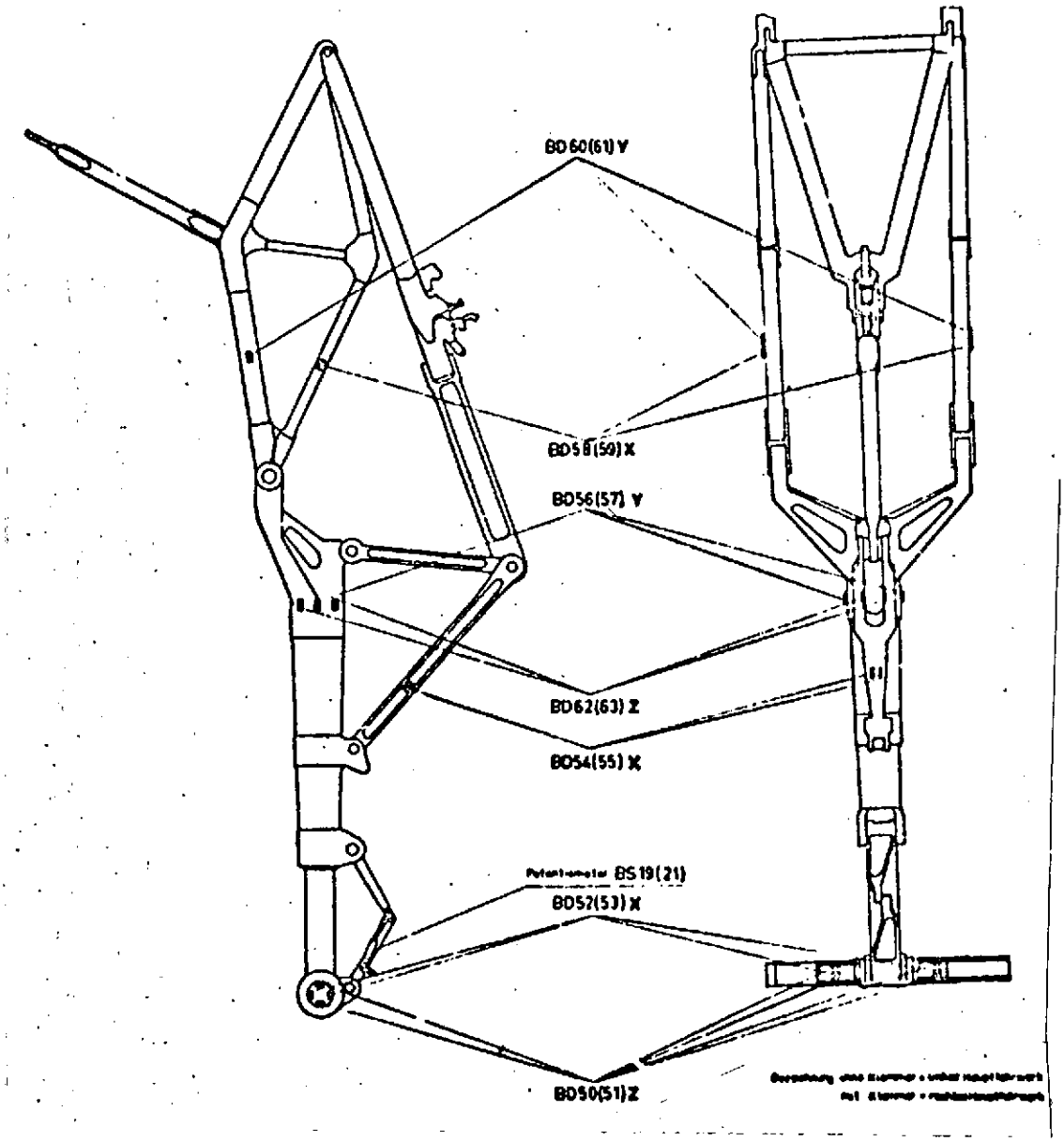

Figure 20. Strain gauges BD on the main undercarriage

REFERENCES

1. Calculation of Dynamic Load Cases. Dornier Report, ZTL Task, No. 53-822-K-4+1.

2. Further Development of Modern Structure Calculation Methods. Dornier Report, ZTL Task, No. TO135/94100/92412.

3. Development of the Transport Aircraft Do 31 and Production and Testing of Two Experimental Aircraft. Dornier Report, GE 51-481/69

   Summary Result Report on the Development Period from 1962 to October 31, 1969.

4. Evaluation of the Landing Sinking Velocity from Flight Measurements for Vertical Landings of the Do 31-E3. Dornier Report, 15031-02.1056

5. Do 31-E1 Measurement of Dynamic Loads on the Nose and Main Undercarriage using Strain Gauges. Dornier Report, EV31-292.

Translated for National Aeronautics and Space Administration under contract No. NASw 2483, by SCITRAN, P. O. Box 5456, Santa Barbara, California, 93108.

STANDARD TITLE PAGE

1. Report No.	2. Government Accession No.	3. Recipient's Catalog No.
NASA TT F- 15,532		

4. Title and Subtitle	5. Report Date
THE DO 31 LANDING LOADS DURING VERTICAL LANDING AND THEIR CONSEQUENCES FOR FUTURE VSTOL DEVELOPMENTS	April, 1974
	6. Performing Organization Code

7. Author(s)	8. Performing Organization Report No.
W. Schoernack	10. Work Unit No.
	11. Contract or Grant No. NASw-2483

9. Performing Organization Name and Address	13. Type of Report and Period Covered
SCITRAN Box 5456 Santa Barbara, CA 93108	Translation

12. Sponsoring Agency Name and Address	14. Sponsoring Agency Code
National Aeronautics and Space Administration Washington, D.C. 20546	

15. Supplementary Notes

Translation of "Die Landelasten der Do 31 bei Vertikallandungen und Folgerungen für zukünftige VSTOL Entwicklungen", Dornier-Werke G.m.b.H., Friedrichshafften (W. Ger.), BMVg-FBWT-72-24; 1972, 72 pp.

16. Abstract

The results of 83 vertical landings carried out during the Do 31 VSTOL Experimental Program are reported. During 23 landings, undercarriage reactions, as well as sinking speeds were measured; of the remaining 60 landings only sinking speeds could be evaluated. Undercarriage reaction factors and sinking speeds are plotted as frequency distributions and discussed. The result of the evaluation of the landing experiments can be summarized as follows: VTOL airplanes of a conception similar to the Do 31 and using manual control during the end of descent would experience considerably higher sinking speeds than conventional aircraft. Furthermore, a typical jumping of the airplane after touchdown and a following second impact prove unfavorable, this second impact resulting in higher undercarriage reactions than the first one. The horizontal loads occurring with vertical landings are smaller than expected.

17. Key Words (Selected by Author(s))	18. Distribution Statement
	Unclassified - Unlimited

19. Security Classif. (of this report)	20. Security Classif. (of this page)	21. No. of Pages	22. Price
Unclassified	Unclassified	52	